ChemComm

FEATURE ARTICLE

View Article Online
View Journal | View Issue

Cite this: *Chem. Commun.*, 2015, **51**, 3957

Received 10th December 2014,
Accepted 2nd January 2015

DOI: 10.1039/c4cc09888a

www.rsc.org/chemcomm

New generation solar cells: concepts, trends and perspectives

Maria-Eleni Ragoussi[a] and Tomás Torres*[ab]

Organic, dye-sensitized and perovskite solar cell technologies have triggered widespread interest in recent years due to their very promising potential towards a high solar electricity future. A number of important milestones have marked the roadmap of each sector on the way to today's outstanding performances, but there still remains plenty of scope for further improvement. The most influential landmarks, together with basic concepts and future perspectives, are unraveled in this review.

1. Introduction

Tackling the global energy crisis is undoubtedly one of the most substantial scientific challenges of our era. Population and economic growth mean constantly increasing energy needs, mirrored primarily in electricity demand, which outpaces all other energy carriers. In addition, the levels of greenhouse gases being emitted in the atmosphere are alarming, confirming that the existing energy trends are problematic, not only from an economic, but also from an environmental point of view. As reported by the International Energy Agency (IEA) in its 2014 Energy Technology Perspectives, current trends in electricity production could have devastating results, extending them to 2050, with energy demand increasing by 70% and CO_2 emissions by 60%.[1] The necessity for a turn towards cost-effective, low-carbon energy technologies is, hence, currently more imperative than ever.

Utilization of renewable sources and particularly solar energy provides, by far, the most solid answer to these questions and the most viable long-term solution. The sun is identified as the most abundant source of energy on earth. As a matter of fact, the solar energy that hits the planet in one hour is equal to the total amount of energy consumed by all human activities in a year.[2] There is no doubt that there is a growing awareness of the urgency for solar energy systems to forge ahead. According to the IEA, an average of 40% annual growth in global photovoltaic (PV) capacity has been observed since 2000. This rapid expansion in

[a] *Departamento de Química Orgánica, Universidad Autónoma de Madrid, 28049 Madrid, Spain. E-mail: tomas.torres@uam.es; Fax: +34 914973966; Tel: +34 914974151*

[b] *IMDEA-Nanociencia, c/Faraday 9, Campus de Cantoblanco, 28049 Madrid, Spain*

Maria-Eleni Ragoussi

Maria-Eleni Ragoussi graduated in Chemistry from the University of Athens (Greece) in 2004, and received her PhD from the University of Birmingham (UK) in 2009. She then joined the group of Prof. Tomás Torres as a postdoctoral fellow. Her research interests involve the synthesis of phthalocyanines and porphyrins for dye-sensitized solar cells, as well as the functionalization of carbon nanostructures for the preparation of electroactive systems.

Tomás Torres

Tomás Torres is Full Professor of Organic Chemistry at the Autónoma University of Madrid (UAM) and Associated Senior Scientist at the IMDEA-Nanoscience. In addition to various aspects of synthetic and supramolecular chemistry his current research interests include the preparation and study of optical properties of organic functional materials. His group, that presently consists of twenty five researchers, is currently exploring several areas of basic research and applications of phthalocyanines, porphyrins and carbon nanostructures (fullerenes, carbon nanotubes, graphene), including organic and hybrid solar cells, with a focus on nanotechnology.

solar energy conversion systems is projected to provide 5% of global electricity consumption in 2030, and 11% by 2050, avoiding, thus, 2.3 gigatonnes (Gt) of CO_2 emissions per year.[3] Put another way, solar power in on the right track to possibly becoming the dominant energy source by 2050, provided that the efforts toward a largely decarbonized energy system continue.[1]

Light energy conversion applications are divided into three categories: photovoltaics (PV) for direct conversion of sunlight into electricity, as well as concentrating solar power systems (CSP),[4] and solar thermal collectors (SHC),[5] employing the sun's thermal energy. The portfolio of photovoltaic applications consists of a number of established as well as emerging technologies. With regard to conventional commercialized modules, crystalline silicon devices, that come in monocrystalline, multi-crystalline and amorphous forms, currently dominate the markets, representing around 90% of the global share.[3] Following the first silicon-based apparatus introduced in the 1950s,[6] research and innovation over the years have led to the current thriving performances. Their broad recognition is attributed to their proven and reliable operation, namely, standard 17–18% efficiency and a lifetime of 20 years.[7] As well, 25% efficiency has been reached by the best to date laboratory Si device.[8] It is noteworthy that some key developments together with the surge in production volumes of silicon PVs have brought about exceptional cost decreases, reaching a 1.00$ per W rate.[9] Similarly, there has been tremendous progress of the inorganic thin film devices, which have proved to be strong competition for silicon PVs, and have also made their way into the market.[10] Modules based primarily on polycrystalline absorber materials, such as cadmium telluride (CdTe) and copper indium gallium diselenide (CIGS) have yielded outstanding performances, reaching efficiencies in the order of 20%. In addition, recently, a device based on indium gallium phosphide (InGaP) yielded an unprecedented 37%.[8] However, this technology is restricted by resource scarcity of the required materials.

In terms of emerging photovoltaic technologies, the current state of the art indicates a vibrant development in recent years. Specifically, organic, hybrid (dye-sensitized) and perovskite solar cells have made remarkable progress and in fact, the first two have hesitantly made their entrance into the market. These new generation devices benefit from low-cost materials, high-throughput manufacturing and low energy expenditure. It is certain, though, that their promising potential for highly efficient energy production remains to be proven.

Herein, we unfold the concepts, advances and perspectives of these innovative solar energy conversion systems that are bound to trigger widespread recognition in the near future.

2. Organic solar cells

Studies on all-organic photovoltaics started as early as the 1950s, when simple organic dyes, like chlorophyll or magnesium phthalocyanines, were investigated, with reported power conversion efficiencies (PCE) not surpassing 0.1%.[11] This poor performance was attributed to the fact that excitons (localized and bound electron–hole pairs), formed upon light illumination, do not dissociate readily in most organic semiconductors, as is the case for inorganic derivatives, and the electrical field developed by the asymmetric work functions of the electrodes in an OPV does not provide the necessary driving force for charge separation.[12] Hence, the main weakness of single-layer architectures was the extensive charge recombination. A significant boost in the OPV performance roadmap came in 1986 when Tang used a two-component donor:acceptor active layer, consisting of a copper phthalocyanine (donor) and a perylene derivative (acceptor).[13] In this case, exciton dissociation at the heterojunction (interface) of the two molecules was favoured due to the substantially different electron affinities and ionisation potentials. A record, for the time, efficiency of 1% was reported.

The donor–acceptor interface can be obtained whether in a planar (PHJ) or bulk heterojunction (BHJ) configuration. In PHJ, the donor and the acceptor are two successively deposited films, whereas in BHJ there is a unique blended film of both components. The great advantage of BHJ in comparison to PHJ is the interpenetrated bicontinuous networks of the components all along the active layer, resulting in a dramatic increase of the contact area and, hence, more efficient charge separation.[12]

The configuration of a device involves a photoactive layer interposed between a modified ITO (indium tin oxide) bottom anode, and a low-work function metal cathode, such as Al, to collect holes and electrons (Fig. 1). To a lesser extent, devices with an inverted structure, that is with an ITO bottom cathode and a high-work function metal anode, have also been studied.[14] The function of a typical OPV system follows four basic steps, as shown in Fig. 1: (1) photoinduced exciton generation, (2) exciton diffusion to the interface, (3) exciton dissociation and hole transfer into the HOMO (highest occupied molecular orbital) of the donor and electron transfer into the LUMO (lowest unoccupied molecular orbital) of the acceptor, (4) charge collection of the electrons and holes at the external electrodes.[15] For this process to take place, fine-tuning of the LUMO orbitals of both donor and acceptor is essential.

The performance of an OPV device is reflected in three parameters: short-circuit photocurrent (J_{SC}), open-circuit voltage (V_{OC}), and fill factor (FF), from which the overall efficiency (PCE) is calculated. The J_{SC} is subject to efficient light-harvesting and carrier generation and mobility, while the V_{OC} is proportional to the energy difference between the HOMO of the donor and the LUMO of the acceptor.[16] In this respect, molecular orbital levels, absorption coefficients, morphology of the layers and molecular diffusion length are the main factors that control the final result. Research in the field has flourished in the last decade and the rational design of new optimized materials has led to PCEs above 10%.[17]

Morphology of the blend at the nanoscale is probably the major challenge in OPVs in an effort to improve charge separation. This being a prerequisite for rationally improving performance, numerous structural characterization techniques as well as physicochemical processing approaches have been developed and carried out on heterojunction films.[18] There are two methods of fabrication: thermal evaporation of active materials under

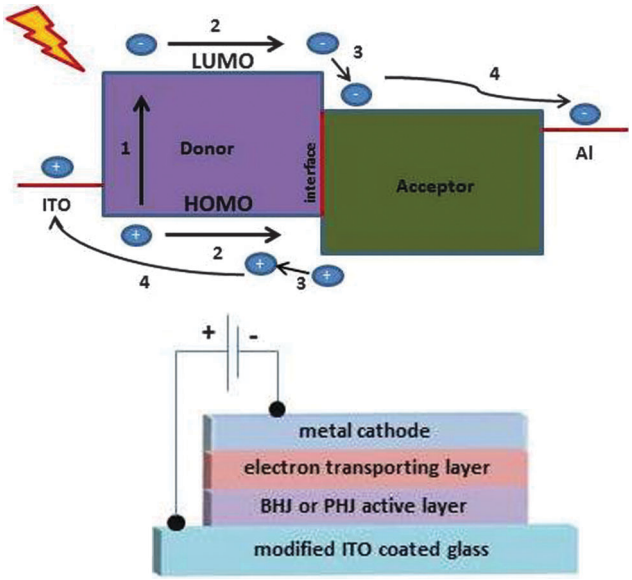

Fig. 1 Operating principles and device structure of an organic photovoltaic system.

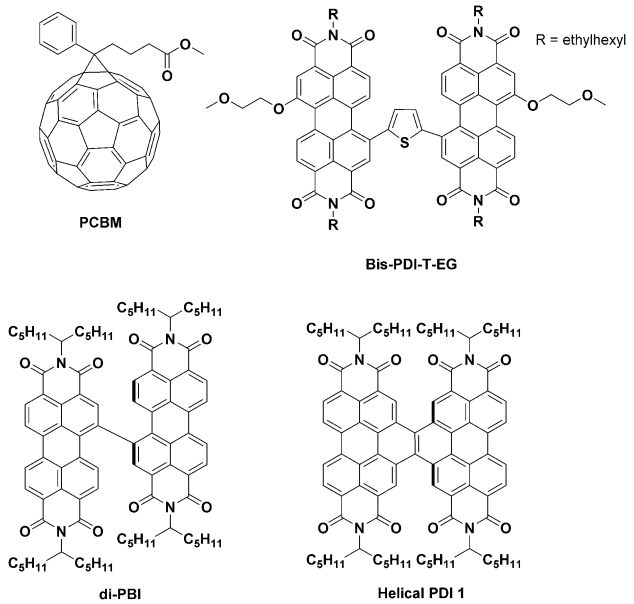

Fig. 2 Structures of electron-accepting components for OPV devices.

vacuum and solution-processing. The latter, applied in preference in polymer OPVs, is simpler, cheaper and offers the possibility to work on large areas of substrates by low energy-demanding technologies. On the other hand, vacuum deposition, used primarily in small molecule-based devices, makes possible the use of insoluble materials often more stable than their soluble analogues, and promotes more precise control of the thickness morphology of the active layers. Both technologies have been used extensively.

2.1 "Plastic" solar cells

"Plastic" solar cell is a term that refers to polymer-based photovoltaics. The most commonly studied systems with the highest efficiencies are BHJ polymer:fullerene combinations, with the polymer acting as the electron donor and the fullerene derivative as the electron acceptor.[19] Fullerenes promote ultrafast charge separation and long exciton diffusion length, and are also characterized by their small reorganization energy and high electron affinity, which renders them ideal electron acceptors.[20] Numerous derivatives have been prepared for OPV applications,[21] but the best performing, and certainly the most popular, is highly soluble phenyl-C61-butyric acid methyl ester (**PCBM**),[22] a benchmark n-type structure for OPVs (Fig. 2).[23] On the other hand, the inherent limitations of fullerenes, namely their narrow absorption in the visible region, low air stability, and high production costs, have triggered the preparation of non-fullerene n-type organic molecules as alternative acceptors for OPVs.[24] Performances, though, remain consistently poor, with the exception of perylenediimides (**PDI**)[25–27] that have shown intriguing behavior and efficiencies of 4–8% (Fig. 2).

In the earliest "plastic OPV" studies, the polymers of choice were poly[2-methoxy-5-(2′-ethyl-hexyloxy)-1,4-phenylenevinylene] (**MEH-PPV**), poly[2-methoxy-5-(3′,7′-dimethyloctyloxy)-1,4-phenylenevinylene] (**MDMO-PPV**) and other PPV-based materials (Fig. 3),[19] but efficiencies did not exceed 3%.[28] The large bandgap of these polymers (over 1.9 eV) did not allow for effective harvesting of photons, which limited significantly further optimization of the device performance. Polythiophenes, and especially poly[3-hexylthiophene-2,5-diyl] (**P3HT** – Fig. 3) subsequently came in the spotlight and performances boosted to 5%,[29] due to better HOMO–LUMO alignment and carrier mobility that resulted in enhanced short-circuit current densities (J_{SC}). Limitations, however, in optimizing the V_{OC} of **P3HT**-based devices[30] shifted interest towards other low-bandgap polymers. Efforts mainly focused on synthetic manoeuvres to tailor their energy levels, not only for effective light-harvesting, but also for better matching of the HOMO–LUMO levels with those of the acceptor for efficient charge transfer. Hundreds of conjugated low bandgap donor–acceptor polymers, based on thiophene, fluorene, carbazole and cyclopentadithiophene among others[17,30] have been synthesized in recent years, and among those, thieno[3,4-*b*]thiophene-based structures have exhibited the most promising behavior, presenting optimally low bandgaps and efficiencies reaching 7–9%.[17] The most successful derivative is polythieno[3,4-*b*]-thiophene-*co*-benzodithiophene (**PTB7**) (Fig. 3), which stands out as the most widely used and best performing polymer in single-junction OPVs.[31] Its very attractive physical characteristics, including bandgap and morphology, have been accounted for the optimal performances, and lately, overall efficiencies reached 9.2%, with a V_{OC} of 0.75 V and an exceptional J_{SC} of 17.46 mA cm^{-2}.[32] Notably, in two hot-off-the-press reports, the 10% threshold was just surpassed with devices based on a **PTB7** derivative (**PTB7-Th**), by applying advanced light manipulation and manufacturing techniques to control photon harvesting and electron mobility.[31c,d]

As well, contrary to HOMO–LUMO level prediction (its bandgap does not match the optimal 1.5–1.7 eV theoretical limits), prototype polycarbazole poly[*N*-9′-heptadecanyl-2,7-carbazole-*alt*-5,5-(4′,7′-di-2-thienyl-2′,1′,3′-benzothiadiazole)] (**PCDTBT**)

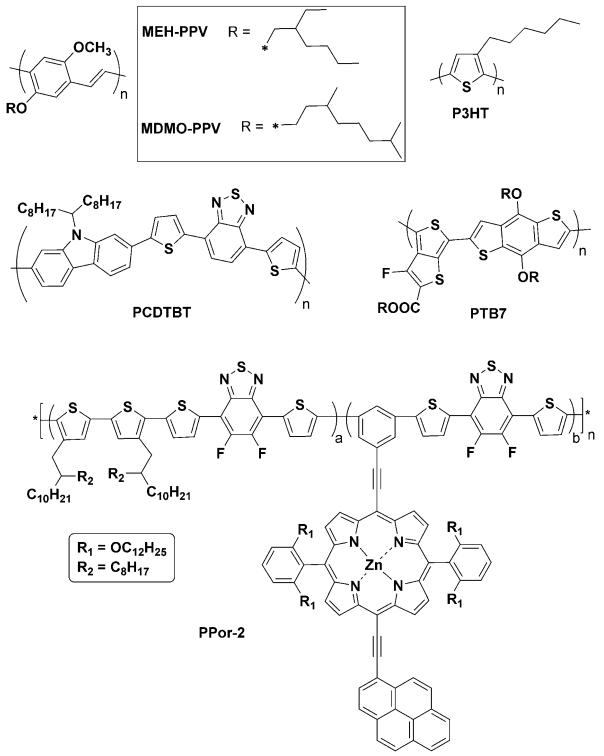

Fig. 3 Structures of successful polymers used in OPV devices.

has attained high performances in the order of 7.5%, with a V_{OC} of 0.90 V (Fig. 3).[33] Its triumphant behavior is attributed to its relatively deep HOMO energy (−5.5 eV), which results in the observed high V_{OC}.[34] Lastly, very recently a co-polymerization approach was described, to produce a panchromatic polymer absorber.[35] Specifically, introduction of a porphyrin–pyrene pendant, endowed with 2,6-bis(dodecyloxy)phenyl substituents to prevent aggregation, on a polythiophene chain gave rise to **PPor-2** which exhibited powerful absorption features and reached a PCE of 8.5% in conjuction with $PC_{71}BM$ (Fig. 3).

2.2 Tandem solar cells

Tandem devices were developed as a means to tackle the limitations of single-junction cells, associated with light absorption and carrier mobilities.[36] Specifically, in standard BHJ devices, the limits in active layer thickness, associated to the low charge-carrier mobilities of most organic materials, do not allow for a maximum amount of photons to be absorbed. Additionally, in multijunction systems, the use of different sensitizers with complimentary absorption spectra allows for coverage of a larger part of the solar flux.

A typical double-junction configuration consists of a front cell with a wide-bandgap material, an interconnecting layer, and a rear cell with a low-bandgap material (Fig. 4). Among the advantages of multijunction devices, reduced thermalization loss of photonic energy and improvement of the open circuit voltage (V_{OC}) are quite intriguing. It is noteworthy that when tandem cells were prepared using the same active materials as Tang in his seminal report,[13] efficiencies twice as high (2.5% PCE), associated to a high V_{OC} of 0.9 V, were observed in a double-heterojunction configuration.[37]

When employing polymers with matched absorption spectra, broader light-harvesting and optimized open-circuit voltage can be accomplished, leading to higher PCEs. It has been reported that the stacking of two or more active layers significantly enhances the theoretical maximum efficiency of a cell under standard illumination, from 30% to 49%.[38] In many cases, when both the single- as well as the tandem-junction architectures were constructed, the latter yielded improved results. Until recently, reported performances had been limited to around 7%, and this was attributed to the use of non-optimized polymers.[39] Nevertheless, lately the 10% threshold was broken with a low bandgap analogue poly[2,7-(5,5-bis-(3,7-dimethyloctyl)-5*H*-dithieno-[3,2-*b*:20,30-*d*]pyran)-*alt*-4,7-(5,6-difluoro-2,1,3-benzothiadiazole)] (**PDTP-DFBT** – Fig. 5), characterized by a bandgap of 1.38 eV, deep HOMO level and high hole mobility.[40] Specifically, an inverted single-junction cell of **PDTP-DFBT**:$PC_{71}BM$ gave a V_{OC} of 0.85 V, J_{SC} of 17.8 mA cm^{-2} and PCE of 7.9%. In a tandem-mode, **PDTP-DFBT**:$PC_{71}BM$ in conjuction with a **P3HT**:Indene-C60Bisadduct(ICBA) (Fig. 5) gave a lower J_{SC} but the V_{OC} rose substantially to reach 1.53 V, which resulted in the extraordinary 10.6% PCE, the highest obtained efficiency in double-junction OPV devices. When two identical **PDTP-DFBT**:$PC_{71}BM$ sub-cells were used, instead, the reported performance was 10.2%.[41]

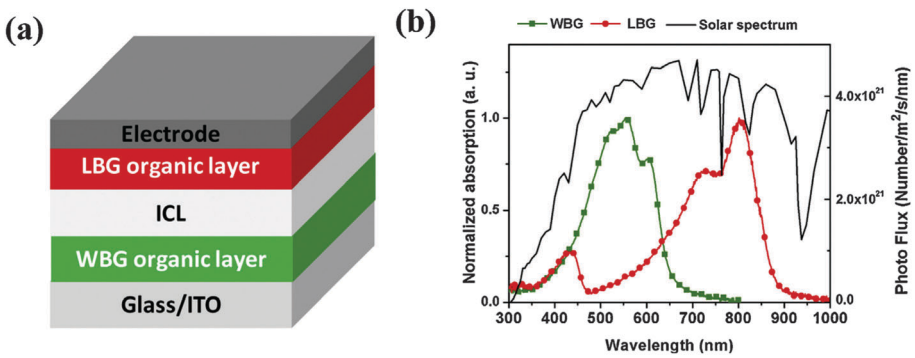

Fig. 4 (a) Configuration of a tandem device, where WBG: wide bandgap material, LBG: low bandgap material and ICL: interconnecting layer; (b) typical wide band gap polymer (green) and low bandgap polymer (red) absorption in comparison with the solar spectrum (black). (Reprinted from ref. 36*d*, Copyright (2013), with permission from Elsevier.)

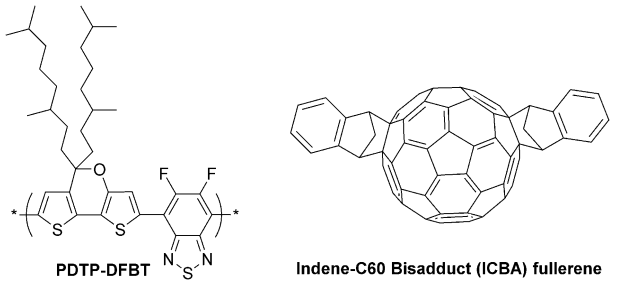

Fig. 5 Structures of polymer **PDTP-DFBT** and ICBA fullerene, used together with P3HT (Fig. 3) in the most powerful double-junction OPV device.

Very recently, a triple-junction device, designed to maximize the photocurrent output, was reported.[42] Specifically, a wide-bandgap (**P3HT** – Fig. 3), a medium-bandgap (**PTB7** – Fig. 3), and a low bandgap donor (**PDTP-DFBT** – Fig. 5), presenting complementary absorption spectra, were stacked under optimized thicknesses, and an outstanding V_{OC} of 2.28 V was observed, yielding an excellent PCE of 11.5%, which exceeds the record efficiency of a double-junction device.[40] Interestingly, it has been suggested previously that triple-junction tandem solar cells tend to achieve higher V_{OC} compared to their double-junction analogues.[43]

Alternatively, very powerful tandem devices have also been prepared using small molecule active materials. It is worth noting that the record in multi-junction architectures is held by Heliatek that recently reported a tandem vacuum-deposited oligomer-based OPV with a certified PCE of 12%.[44] Additional examples of small-molecule tandem architectures are discussed within the next chapter.

2.3 Small-molecule heterojunctions

In spite of the plentiful advantages of polymers employed as the light harvester and electron donor in OPVs, limitations related to the reproducibility of their synthesis, purification, and inherent electronic properties sparked the search for alternatives, and the most promising solution lies in small conjugated molecules. Research in the field was initiated in 2006,[45] and since then the synthesis of many classes of chromophores, such as oligothiophenes, triphenylamines, borondipyrromethene (BODIPY) diketopyrrolopyrroles, porphyrins, phthalocyanines and other π-conjugated molecules has been described.[46–48] As mentioned earlier, the most commonly used processing technique in small-molecule OPVs is vacuum deposition, as a means to enhance charge transport capabilities and overcome insolubility phenomena. Solution processing (spin-coating, inkjet printing, dip-coating, spraying technique) has, however, also been employed, giving rise to a vast number of successful configurations.[49]

Oligothiophenes are among the most-studied organic semiconductors, owing to their intriguing charge transport characteristics and tunable optoelectronic properties.[50] Initial studies in vacuum-deposited OPVs focused on 3D oligothiophenes, such as **1** (Fig. 6), but low efficiencies, attributed to the poor absorption characteristics of the material, were generally observed.[46,47a] A number of other oligothiophene analogues and configurations have been prepared and tested,[48] with the best performance being reported recently by Bäuerle and co-workers with a novel

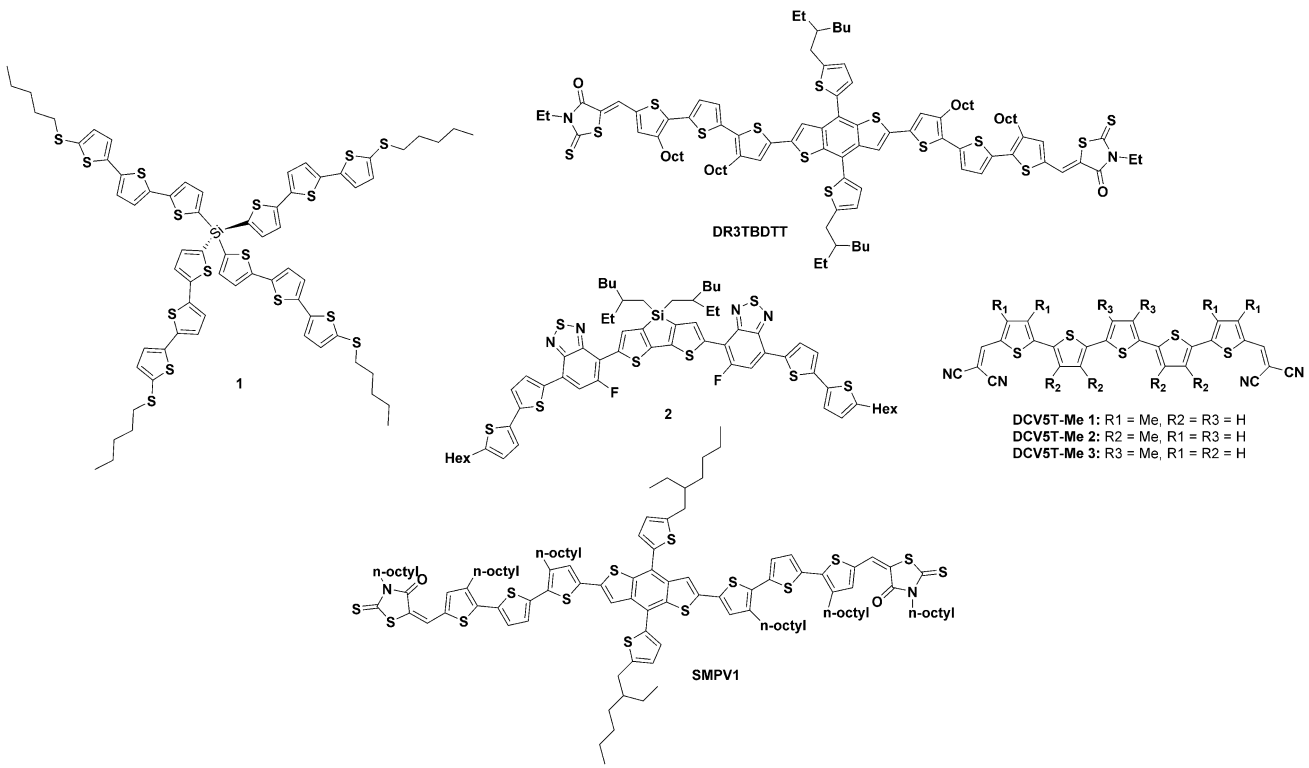

Fig. 6 Structures of oligothiophene-based dyes used in vacuum- and solution-processed OPVs.

series of methyl-substituted dicyanovinyl quinquethiophenes (**DCV5T-Me 1–3** in Fig. 6).[51] BHJ thin film devices were prepared using the new dyes as the electron donor and C60 as the acceptor counterpart and gave rise to outstanding PCEs (4.8% for the **1**- and **2**- based devices and 6.9% for the **3**-based one, under optimized conditions). In this case, the high crystallinity of the photoactive blend layer was accounted for the exceptional outcome. In terms of solution-processed oligothiophene-based OPVs, a significant boost has been observed in performance. Rational design for optimization of the V_{OC} and J_{SC} led to the very promising derivatives **2** and **DR3TBDTT** (Fig. 6). The molecular design consisted of adopting greater conjugation to achieve improved light-harvesting and hence J_{SC}, and long alkyl chains to enhance solubility. Solar cells fabricated with the architecture ITO/PEDOT:PSS/**2**:$PC_{71}BM$/Ca/Al showed PCE values of 7%,[52] and those with ITO/PEDOT:PSS/**DR3TBDTT**:$PC_{71}BM$/LiF/Al gave 8.12% (V_{OC}: 0.93 V and J_{SC}: 13.17 mA cm^{-2}), which are the highest, to date, reported efficiencies for small-molecule single-junction OPVs.[53] With regard to oligothiophene tandem devices, an exceptional system was constructed very recently, and was featured with polythiophene **SMPV1** as the chromophore (Fig. 6), in conjuction with $PC_{71}BM$.[54] In a single junction, the solution-processed device, with **SMPV1**:$PC_{71}BM$ as the active layer, exhibited a certified power conversion efficiency of 8.02%, while the homo-tandem architecture gave a record PCE of 10.1%, with a remarkable V_{OC} of 1.82 V and FF of 72%. The origin of the enhancement was suggested to be the increased optical absorption.

Among other organic dyes, intriguing results have been observed with oligoacenes, and particularly pentacene **3**[55] and rubrene **4**,[56] reaching efficiencies around 3%, and squaraine dyes, such as **5**, with a 3.10% highest reported PCE (Fig. 7) in vacuum-evaporated systems.[57] The same dye, **5**, was later used in a solution-processed device, with $PC_{71}BM$ as the acceptor counterpart, and the efficiency rose to 5.20%.[58] Squaraines present several interesting features, such as high extinction coefficients, photochemical stability and possibility to design other small molecular structures. Additionally, triphenylamine-based derivatives, such as **8**, (Fig. 7), singled out for their high absorption coefficients in the 600–700 nm regime, have yielded among the finest reported performances for vacuum-deposited hybrid heterojunction (HHJ) cells (J_{SC}: 13.48 mA cm^{-2}, V_{OC}: 0.93 V and PCE: 6.80%).[59] Efficiencies in the order of 6% have been reported with merocyanines (Fig. 7, compound **6**) in a thin film, single-junction architecture.[60] Remarkably, in a tandem configuration using merocyanine **7** as the active molecule in two identical sub-cells, an extraordinary V_{OC} of 2.10 V was accomplished, leading to a 4.80% PCE.[61] Lastly, a donor–acceptor–acceptor (D–A–A) structure, based on an electron-donating ditolylaminothienyl moiety, connected to an electron-withdrawing dicyanovinylene *via* a pyrimidine group, was recently prepared and studied in vacuum-processed devices, bringing about remarkable results (Fig. 7).[62] In particular, optimized **DTDCTP**:C70 PHJ architectures gave a PCE of 6.4% with a V_{OC} of 0.95 V, J_{SC} of 12.1 mA cm^{-2} and FF of 0.56. The impressive V_{OC} was attributed to the low-lying HOMO level (−5.46 eV) of the donor material.

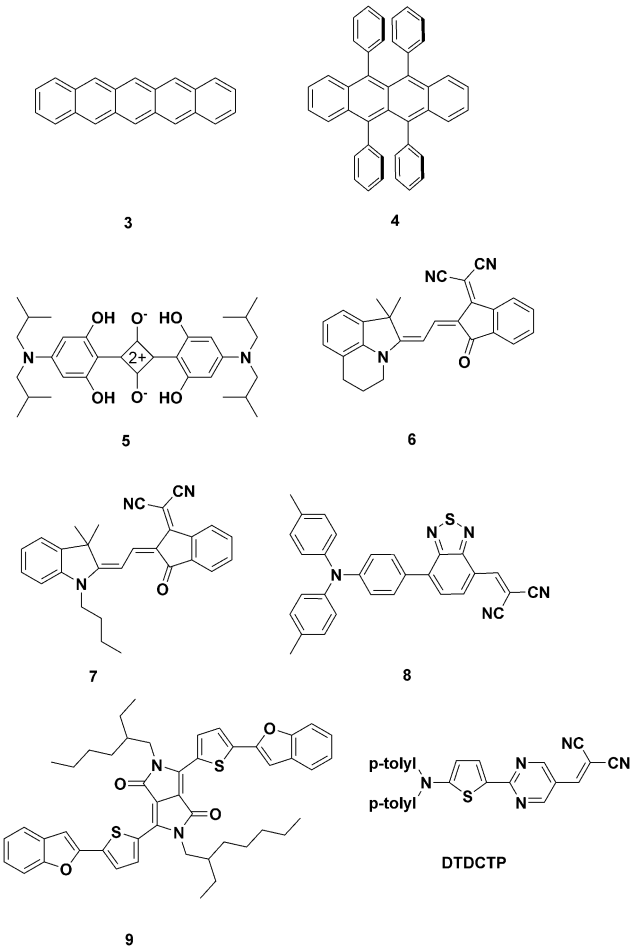

Fig. 7 Structures of small molecules used in vacuum- and solution-processed OPVs.

Noteworthy are also the results that have been obtained with diketopyrrolopyrroles (DPP) in solution-processed systems. DPP are attractive building blocks in terms of synthetic versatility. Modification of the main structure with benzofuran substituents led to derivative **9** (Fig. 7), that exhibited increased intermolecular chromophore interaction through high conjugation as well as stabilized HOMO levels.[63] In detail, a deep HOMO of −5.2 eV was observed and when blended with $PC_{71}BM$, it gave a V_{OC} higher than 0.9 V, a J_{SC} of 10 mA cm^{-2} and an overall efficiency of 4.4%.

From a different angle, notwithstanding the great success of porphyrins in dye-sensitized solar cells, as this will be discussed further down, this class of compounds has not been as triumphant in OPVs due to their reduced absorption in the red region of the visible spectrum and the lower charge-carrier mobility and exciton–diffusion length of the evaporated films.[47b] In terms of phthalocyanines, several examples of planar heterojunction architectures have been described, enticed by the attractive features of these macrocycles, namely their high extinction coefficients in the visible region, rich redox chemistry and photostability. An interesting development came by combining a vacuum-deposited Cu(II)Pc/C60 thin film in a

ITO/PEDOT:PSS/Cu(II)Pc/C60/BCP/Al format, obtaining 4.2% PCE under 4.4 suns.[64] An impressive enhancement was observed when the same active materials were used in a hybrid heterojunction (HHJ) geometry, attaining 5% PCE.[65] As well, a tandem configuration consisting of two HHJ stacked in series, brought about a further increase in PCE to 5.7%.[66]

Along the same lines, one of the most uprising molecules in the area of OPVs is subphthalocyanines (SubPcs).[67] This phthalocyanine analogue can be used both as the molecular donor and acceptor of the device. In this regard, SubPc **10**:C70 architectures have achieved 5.4% efficiencies in vacuum-deposited systems (Fig. 8).[68] Alternatively, fullerene-free cells consisting of SubPc **10** as the donor and perchlorated SubPc **11** as the acceptor have accomplished PCEs of 2.7%.[69] The good performance in this case was attributed to the increased V_{OC} compared to a similar SubPc–C60 combination. Interestingly, when the same powerful SubPc acceptor **11** was paired with subnaphthalocyanine **12** as the donor counterpart in a SubNc **12**:SubPc **11** configuration, the outstanding 6.4% was reported (Fig. 8).[70] The result was rationalized on the basis of complementary absorption of the two subphthalocyanine analogues, the reduced recombination at the interface and the improved energetic alignment. These are the so-called ''all SubPc based-devices''. Lastly, when **10** and **12** were used both as acceptors in a three-layer vacuum-processed architecture with an α-sexithiophene (α-6T – compound **13**, Fig. 8) as the donor, a record (in fullerene-free systems) 8.4% efficiency was accomplished.[71]

Briefly, the evolution of organic photovoltaics in the last two decades can be described through a number of vital landmarks. Undoubtedly, Tang's introduction of the two-component donor:acceptor active layer was the beginning of a thriving era in the field.[13] Further improvements led to the bulk heterojunction configuration that brought about significant increases in the overall performance of the cells.[18] In terms of materials, a number of polymers, such as **PPV**-based,[19] **P3HT**[29] and **PTB7**[31] set important milestones on the way to today's state-of-the-art in electron-donor structures. Lately, a new polymer, **PDTP-DFBT**,[40] as well as polythiophene **SMPV1**,[54] have established new landmarks, by overcoming the 10% efficiency threshold, in tandem-mode devices. As regards electron acceptors, the most important development consists of fullerene derivative phenyl-C61-butyric acid methyl ester (**PCBM**)[22,23] which has been the most successful and widely used analogue.

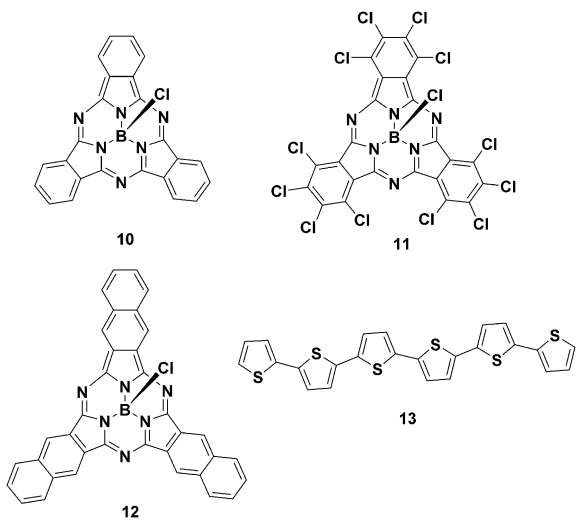

Fig. 8 Structures of donor and acceptor subphthalocyanine analogues and **a-6T** donor for OPVs.

3. Dye-sensitized solar cells

The development of dye-sensitized solar cells (DSSCs) in the 1990s opened up new horizons in the area of photovoltaics, and entered dynamically the race for cost-efficient devices functioning at the molecular level.[72] This pioneering architecture was introduced by O'Regan and Grätzel[73] and has shown a tremendous potential as an alternative to the standard silicon photovoltaics,[74] with the obtained efficiencies growing from 7% in the seminal report[73] to 13% recently.[75] A wealth of active components and configurations has been developed since and the field has been growing fast. The low production costs combined with the attractive technical features of DSSCs – such as transparency, ease of processing, stability and solidity over wide temperature ranges[76] – have constituted the driving force for the overwhelming attention that the field has received over the past years. As well, the standards for material purity are much lower, meaning that processing under vacuum and high temperatures is not required.[77]

The working principle of DSSCs differs substantially from that of OPVs and is, instead, closely related to natural photosynthesis. Concretely, the fundamental processes, as those are illustrated in Fig. 9, include:

1. Photoexcitation of the sensitizer,
2. Electron injection into the conduction band of the metal oxide (TiO_2),
3. Electron transport to the working electrode,
4. Regeneration of the oxidized dye by electron donation from the redox couple of the electrolyte.

The photogenerated electrons at the anode flow through an external circuit to reach the counter electrode, where the oxidized redox couple is regenerated (process 8 in Fig. 9). Additionally,

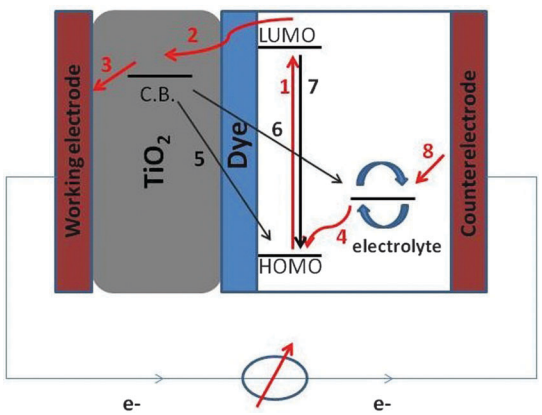

Fig. 9 Operating principles of dye-sensitized solar cells.

other than the desirable phenomena that take place during the operation of a DSSC, there are also competing processes that involve recombination of the injected electrons either with the oxidized dye (process 5 in Fig. 9) or with the redox couple (dark current – process 6 in Fig. 9). Alternatively, the excited dye may also relax to its ground state by a non-radiative decay process (process 7 in Fig. 9).

Research for optimal technology progress in DSSCs focuses on tailoring the physicochemical properties of the three main components of the cell: (i) the organic dye, (ii) the nanocrystalline semiconductor and (iii) the redox couple in the electrolyte. For a device to be successful, all components require fine-tuning.[78]

3.1 Organic dye

The sensitizer is probably the key element in a DSSC device, since it governs the photon harvesting, charge generation and charge transfer processes. Several thousands of photosensitizers have been investigated over the years and numerous synthetic strategies have been developed looking to optimize dye requirements, namely suitable energy levels for charge injection and dye regeneration, appropriate anchoring group to attach to the semiconducting material and broad absorption in the visible and NIR region.[79] Historically, ruthenium-based photosensitizers, and in particular **N3**,[80] its salt analogue **N719**,[81] and **N749** (black dye)[82] marked significant breakthroughs, with PCEs reaching 10–11% and incident photon to current conversion efficiency (IPCE) of 80% across the visible part of the solar spectrum (Fig. 10). Interest in ruthenium dyes stems from their wide absorption range in the visible and NIR range, thermal and photostability and excellent charge transfer properties. Advancements in their molecular design[83] focused mainly on the addition of p-conjugated systems to the main bipyridyl ligand in an effort to enhance light harvesting, and in this respect, today's most successful analogue, that is **CYC-B11** (Fig. 10), stands out for its conjugated thiophene chains and high molar extinction coefficient, yielding a PCE of 11.5%.[84]

The synthetic focus later shifted towards other organic sensitizers, largely driven by the need to produce Ru-free materials in order to bypass not only the limitation of their high cost, but also their usually poor absorption extinction coefficients. Many different organic dyes, such as indolenes, perylenes, squarines, donor–acceptor (D–A) dyes, have been reported over the years, but efficiencies consistently remain in the range of 6–8%[85] with a few exceptions. The best performing metal-free organic sensitizers to date are D–A dyes **C219**, with a 10.1% PCE[86] and **RK1** with 10.2% (Fig. 11).[87]

Along the same lines, much attention has been drawn around porphyrin sensitizers (Pors),[88] which has marked the emergence of the best performing sensitizer to date in DSSCs.[75] Their large absorption coefficients in the visible region of the solar spectrum together with the great possibilities of molecular engineering have been the driver that boosted this vivid interest and the myriad of studies that enabled the benchmark efficiency to increase to 13%. ''Push–pull'' porphyrin **YD2-oC8** (Fig. 12) was based on a pivotal molecular design for slowing the rate of

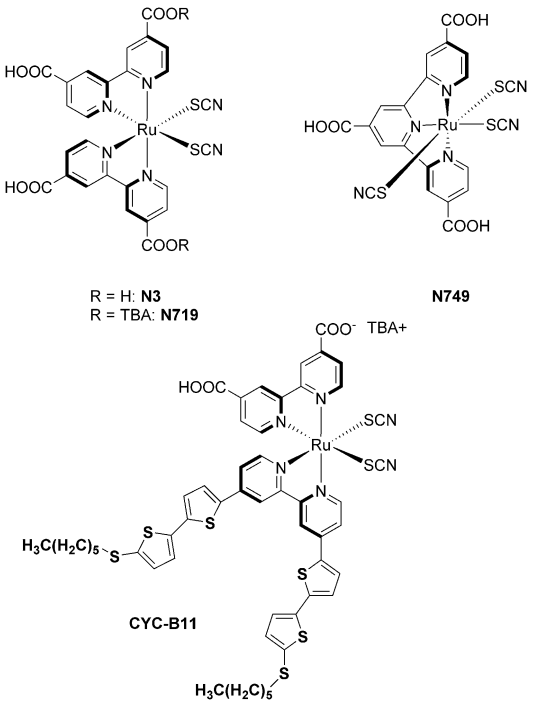

Fig. 10 Structures of Ru-sensitizers used in DSSCs.

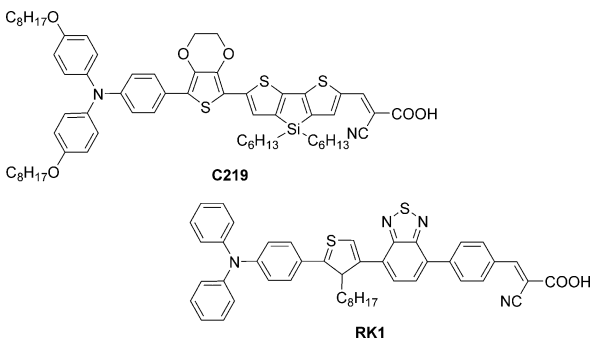

Fig. 11 Structures of organic dyes used in DSSCs.

charge recombination that was the introduction of long-chain alkyloxy groups in the main scaffold. As a result, a V_{OC} of nearly 1 V was attained, leading to a PCE of 11.9%.[89] Further improvements in the structural optimization of Por dyes involved the introduction of benzothiadiazole (BTD) as an electron acceptor, which yielded porphyrins **GY50**[90] and **SM315**[75] (Fig. 12). The addition of the BTD was successful in filling the gap between the Soret band and the Q band in the absorption spectrum, giving rise to panchromatic sensitizers. An excellent V_{OC} of 0.88 V, a J_{SC} of 18.53 mA cm^{-2} and a PCE of 12.75% were observed for **GY50**, while **SM315** broke the DSSC efficiency record with V_{OC}: 0.91 V, J_{SC}: 18.1 mA cm^{-2} and PCE: 13.0%.

In terms of Pc-sensitized solar cells, the performance of the existing devices has not yet achieved the levels of porphyrins, however tremendous progress has taken place recently.[91] Building on their excellent light-harvesting properties in the far red- and near IR spectral region and their extraordinary robustness, Pcs have been established among the benchmark dyes in the field.

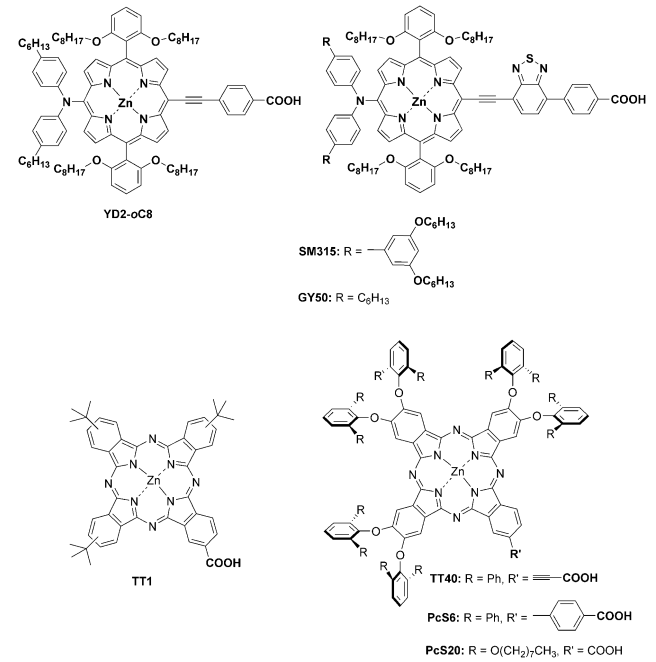

Fig. 12 Structures of porphyrin and phthalocyanine dyes used in DSSCs.

The renaissance of these macrocycles in DSSC applications came first with the use of bulky *t*-butyl groups in the periphery of the scaffold, as a means to supress molecular aggregation, one of the main challenges in device optimization. In this context, Pc **TT1** reached 3.5% overall efficiency (Fig. 12).[92] The utilization of even bulkier diphenylphenoxy substituents, brought about a significant boost in the performance, first with **PcS6** yielding a 4.6% PCE[93] and later with **TT40** with 6% (Fig. 12).[94] The diphenylphenoxy groups, in this case, act not only by avoiding macrocycle aggregation, but also, by blocking the interactions between the Pc and the electrolyte, reducing the so-called catalysis of recombination and unwanted dark currents.[95] Replacement of these bulky phenyl-based substituents by long alkyl chains led to the most successful Pc dye to date, **PcS20** (Fig. 12). An excellent 6.4% PCE under 1 sun illumination was reported, which was attributed to increased dye adsorption density.[96]

3.2 Liquid electrolytes *versus* solid hole transporting materials

There are two main directions on DSSC research towards the optimization of device performance: one is to extend the light-harvesting region of the organic sensitizer into the near-infrared (NIR), this way enhancing J_{SC}, and the other to lower the redox potential of the electrolyte in order to increase the V_{OC}.[78] The design of electrolytes is, thus, of strong priority. The most popular redox couple is I^-/I_3, the key to its success being the slow recombination reaction.[97] However, certain limitations stem from its corrosive nature and complex two-electron redox chemistry. Several alternative redox couples have been discovered, including Br^-/Br_3,[98] LiBr/Br_2[99] and hydroquinone-based,[100] but gave unimpressive results due to unacceptably high recombination rates. Successful performance was, however, observed with novel ferrocene Fc/Fc^+,[101] all-organic[102] and principally Co^{2+}/Co^{3+} electrolytes. As a matter of fact, cobalt-based electrolytes are the high point as a powerful alternative to their iodine-based analogues. The first blooming example, tris(2,2′-bipyridyl)cobalt(II/III), was reported in 2010 by Feldt *et al.*,[103] and was followed by a number of other engineered complexes, mostly based on 2,2′-bipyridine (bpy),[104] phenanthroline[105] and polypyridyl[106] ligands. An attractive feature of cobalt complexes is that their electronic properties and redox chemistry can be strategically tuned by varying the ligand environment. It is noteworthy that all the latest accomplishments in porphyrin-sensitized devices have been obtained using the cobalt redox mediator $Co(bpy)_3$.[75,89,90]

Alternatively, huge progress has also been seen in the development of solid hole conductors. There are some inherent limitations of liquid electrolytes, associated with leakage, corrosiveness and volatility, which pose a major challenge in the mass production of DSSCs. In this regard, the development of solid hole-transporting materials (HTM) towards the preparation of all-solid-state hybrid devices (ss-DSSCs)[107] has attracted vivid interest. In ss-DSSCs, hole transfer occurs directly from the oxidized dye to the HOMO of the HTM, which then transports the charge to the counterelectrode.[108] Initial studies on ss-DSSCs did not manage to exceed 1% efficiencies, but recently this value has increased to 10.2%.[109] In any case, despite the significant progress, performances have not yet made it to be at par with those of their liquid electrolyte analogues. Several organic and inorganic materials have been proposed as hole-transporters, with the highest V_{OC} values being obtained in devices that employ a small-molecule hole conductor.[110] The best-performing HTM is triphenylamine-based spiro-MEOTAD[111] (Fig. 13) in organic-based materials, giving an overall efficiency of 7.2% when paired with **Y123** dye (Fig. 13),[112] and $CsSnI_3$ in the inorganic analogues, reaching 10.2% in conjunction with **N719** dye (Fig. 10).[109]

Current solid hole transporting materials face some major challenges that limit the enhancement of device performance. On one hand they are characterized by poor light harvesting capabilities and low internal quantum efficiencies, which lead to J_{SC} values lower than liquid-based DSSCs. On the other hand, even though they are fabricated through solution processed techniques, pore-filling can never be complete because space is left when the solvent evaporates, a fact that greatly influences morphology and thus, charge separation and collection.

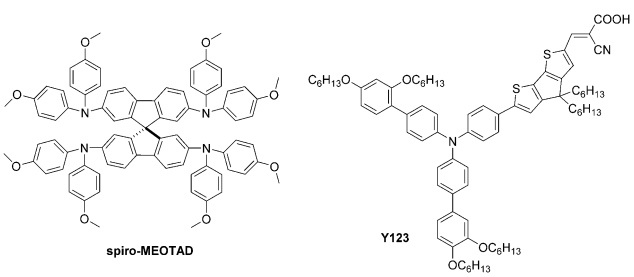

Fig. 13 Structures of HTM spiro-MEOTAD and organic dye Y123.

3.3 Other strategies

The key to the flourishing of DSSCs in the 1990s was the use of a mesoporous TiO_2 electrode,[113] a low-cost material that can be processed in transparent flexible films of large interfacial area and allows a high load of dye. Another important feature was its high electron mobility. A number of other oxides, such as ZnO,[114] SnO_2,[115] and Nb_2O_5,[116] have been tested as alternatives, but TiO_2 has overall given the highest efficiencies by far, which is why it is still the most commonly used metal semiconductor.

In a different aspect, one of the fundamental strategies to enhance light-harvesting, is by achieving panchromatic absorption through co-sensitization with dyes possessing complementary optical properties.[78,117] Even though certain constraints can occur due to intermolecular interactions between the dyes that decrease the injection dynamics,[118] several optimal combinations have been developed. The most powerful one was described recently and was based on a porphyrin–organic dye couple [**YD2-oC8–Y123**] (Fig. 12 and 13).[89] The lack of absorption of the porphyrin in the 480–630 nm range was complemented by **Y123**, which exhibits an absorption maximum at 532 nm and high extinction coefficient. The co-sensitized cell resulted in the J_{SC} climbing to 17.66 mA cm^{-2} and the PCE reaching 12.3%. Similarly, another promising strategy for panchromatic engineering relies on the use of energy relay dyes (ERDs). Their operating principle is to absorb light and then proceed to non-radiative energy transfer, typically Förster resonant energy transfer,[119] to the organic sensitizer that is responsible for charge separation.[120] In this case, light-harvesting is decoupled from charge-transfer, which brings about a range of advantages over co-sensitization techniques. For instance, since ERDs do not participate in the charge-transfer process, precise control of their energy levels is not necessary, meaning that a broad range of dyes can play this role. As well, they do not require attachment on the TiO_2 surface and thus, do not affect the dye loading, and also, the use of multiple ERDs to expand the overall spectral coverage is possible.[121] Along these lines, several analogues have been described, such as perylene derivative, **PTCDI**,[120] 4-(dicyanomethylene)-2-methyl-6-(4-dimethylaminostyryl)-4*H*-pyran (**DCM**)[122] and recently benzonitrile soluble **BL302** and **BL315**,[123] which in **TT1**-sensitized solar cells (Fig. 12) gave overall efficiencies of a maximum of 4.5%.[122]

Overall, research in the area of DSSCs has been marked by a number of important milestones. Following the prominent article by O'Regan and Grätzel in 1991 introducing this novel technology,[73] a number of outstanding Ru-dyes came in the spotlight for breaking the 10% barrier in efficiency,[80–82] and more recently two remarkable well-designed porphyrins set a new landmark, by eliminating the need for rare and costly ruthenium based sensitizers as a requirement for high efficiencies (Fig. 14).[75,89] As well, the introduction of Co-based electrolytes has been one of the key players in advancing device construction,[75,89,90,104] as has the development of solid electrolytes, giving access to all-solid-state devices,[107] a prerequisite in the race for commercialization.

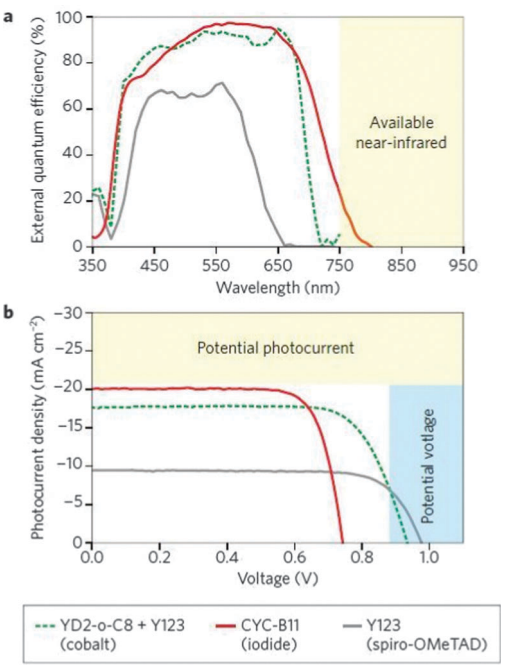

Fig. 14 (a) External quantum efficiency (EQE) *vs.* wavelength and (b) J_{SC} *vs.* V_{OC} of some of the most successful combinations of dye–electrolyte: CYC-B11/iodide redox couple (red line), co-sensitized (YD2-o-C8 and Y123)/cobalt redox couple (green line) and Y123 dye/solid-state hole conductor spiro-OMeTAD (grey line). Reprinted by permission from Macmillan Publishers Ltd: [*Nature Photonics*] (ref. 78), copyright (2012).

4. Perovskite solar cells

The latest trend in photovoltaics has been perovskite-sensitized solar cells.[124] The field has grown in a ballistic manner in the last years and efficiencies rapidly surpassed those of all other organic or hybrid solar cells. It is noteworthy that perovskite-based devices were selected among the breakthroughs of the year 2013.[125] The operating principles are not yet well-understood, but speculation and studies suggest that they work differently than DSSCs even though their configuration is similar, and that indeed, they represent a new type of solar energy conversion systems. The main advantage of perovskite solar cells is their ability to perform all three basic tasks required for solar cell operation: light harvesting, charge generation and transport. In addition, their absorption coefficients can be as high as one order of magnitude greater than ruthenium complexes, and they feature long-range charge transport properties. As a matter of fact, they appear to overcome the hurdles of DSSCs, and offer, at the moment, the greatest paradigm for potential substitutes of Si-based and inorganic thin film modules.

Perovskites can be represented as an AMX3 octahedral structure (A = Ca/K/Na/Pb/Sr/*etc.*, M = metal cation, X = oxide/halide anion), where M occupies the center and is surrounded by X located at the corners (Fig. 15). In turn, A fills the hole formed by the eight octahedra in the three-dimensional structure, and also balances the charge of the system. Perovskites can be, other than purely inorganic, also organic–inorganic,

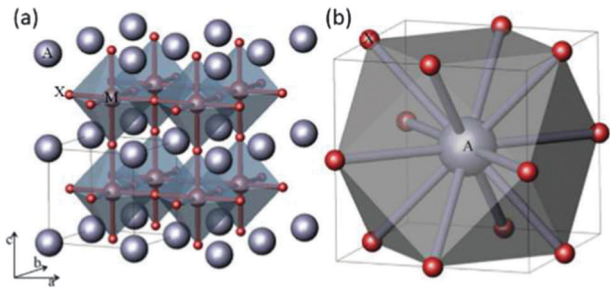

Fig. 15 Perovskite structure (a) crystal structure of cubic perovskite of general formula AMX3; (b) twelve-fold coordination of the A-site cation. Adapted from ref. 124c with permission from The Royal Society of Chemistry.

in which case A is an organic cation, such as alkyl or aryl ammonium. The inorganic analogues are among the most abundant minerals in nature.[126] The wide bandgap characterizing perovskites can be engineered by modifying one or more of the components of the structure.

Organo-lead perovskite analogues, and mostly RNH_3PbI_3, have been the light-harvester of choice in most cases, due to their large absorption coefficients and high carrier mobilities.[124c] The first devices based on mesoporous TiO_2 photoanodes were reported in a pioneering work from Miyasaka and co-workers in 2009. In particular, sensitization of the metal oxide with $CH_3NH_3PbI_3$ in a liquid electrolyte yielded moderate PCEs of 3.81%, yet an intriguingly high V_{OC} of 0.96 V.[127] Optimization of the titania surface and utilization of $CH_3NH_3PbI_3$ quantum dots quickly improved the performance to 6.5%.[128] Poor stability of perovskites being one of the main obstacles towards further enhancements, the addition of a protective Al_2O_3 layer to prevent corrosion by contact with the electrolyte was suggested, and indeed, 6% efficiencies were reported under this strategy.[129] Replacing the liquid electrolyte by a solid hole transporting material seemed like a more robust solution to this problem, and this, in fact, has been reflected in a recent surge in the development of solid-state devices. Tremendous progress in the area has, indeed, resulted in unique efficiencies currently reaching 20.1%, according to the latest chart on record cell efficiencies from the National Renewable Energy Laboratory (NREL).[130]

Several milestones are noteworthy in the perovskite roadmap: a 10.4% overall efficiency was reported for a $CH_3NH_3PbI_3$-sensitized cell with a spiro-OMeTAD HTM, dopped with tris[2-(1*H*-pyrazol-1-yl)-4-*tert*-butylpyridine]cobalt(III)tris[bis(trifluoromethylsulfonyl)imide] (FK209), yielding a J_{SC} of 18.3 mA cm^{-2}, and a V_{OC} of 0.865 V.[131] The HTM-free cells were also an influential discovery, since they showed that perovskites can act both as the light-harvester and the HTM counterpart.[132] This technology has reached an 8% PCE with a $CH_3NH_3PbI_3$–TiO_2 combination. A different configuration consisted in a TiO_2-free device, with novel $CH_3NH_3PbI_2Cl$ sensitizer, exhibiting better stability and carrier transport than the pure iodide equivalent, which boasted an extraordinary 10.9% PCE and an overwhelming 1.1 V V_{OC}.[133] In this case the perovskite acted both as a sensitizer and electron-transporter and a mesoporous alumina scaffold was used to absorb the sensitizer.

One of the most astounding developments in the field was the sequential deposition method for the fabrication of perovskite-sensitized TiO_2 films. In contrast to past deposition methods that involved uncontrolled precipitation of the perovskite and lead to varying morphologies, Grätzel and co-workers introduced a two-step sequential method in which a concentrated PbI_2 solution was first spin-coated, followed by CH_3NH_3I deposition by dip-coating to form $CH_3NH_3PbI_3$ perovskite. This allowed them to homogenize the morphology of the system.[134] Their methodology was rewarded with a record 14.1% obtained PCE, which is among the highest-reported performances to date.

The preparation of planar heterojunction perovskite devices was the next achieved landmark.[135] Studies on nanostructured DSSC-like devices, replacing TiO_2 by Al_2O_3, not only attained impressive efficiencies in the order of 12%, but also gave substantial proof suggesting that the perovskite possesses unique ambipolar properties to transport both photogenerated holes and electrons.[133,136] These findings served as a base to proceed with the construction of simplified vapour-deposited heterojunction architectures, with $CH_3NH_3PbI_{3-x}Cl_x$ as the absorber, a compact layer of n-type TiO_2 as the electron collecting layer and spiro-OMeTAD as the HTM, attaining 15% PCE, with a J_{SC} of 21.5 mA cm^{-2} and a V_{OC} of 1.07 V.[135] The deposited films were extremely uniform at the nanometer scale, as opposed to solution-processed films, and this was the rationalization behind this outstanding performance. Efficiencies climbed to 15.7% when a thin film of ZnO nanoparticles was used as an electron-transport layer.[137] These results were obtained with methyl ammonium lead triiodide (MAPbI3), which boasts excellent light-harvesting features: a narrow band gap of 1.55 eV, high extinction coefficient and outstanding incident-photon-to-current conversion efficiency (IPCE) until 800 nm, harvesting photons from the visible range to part of the near-infrared (Fig. 16).[127,128,137]

Replacement of methylammonium in MAPbI3 by slightly larger formamidinium, affords the $FAPbI_3$ derivative, characterized by a 1.45 eV bandgap, which leads to broader absorption, as well as high photostability. This material has yielded very promising results,[138] with the latest efficiencies very recently reaching 16.01%.[139] Alternatively, a fabrication approach based on the rigorous control of the perovskite film processing in planar heterojunction architectures and controlled humidity conditions, achieved to suppress recombination and enhance carrier injection, resulting in the second highest, to date, reported efficiency of 19.3% in the field.[140]

Similarly, a fully solution-processed cell, based on a bilayer architecture that featured characteristics of both mesoscopic and planar structures, gave rise to a certified 16.2% power-conversion efficiency.[141] The described method managed to produce extremely uniform and dense layers of the active $CH_3NH_3PbI_{3-x}Br_x$ perovskite material that absorbed incident light very efficiently.

In a different aspect, the exploration of other HTM systems, different than spiro-OMeTAD has led to a number of interesting results, among which was the incorporation of polymers PCDTBT, P3HT or poly(triarylamine) (PTAA) in CH_3NH_3PbX-based cells

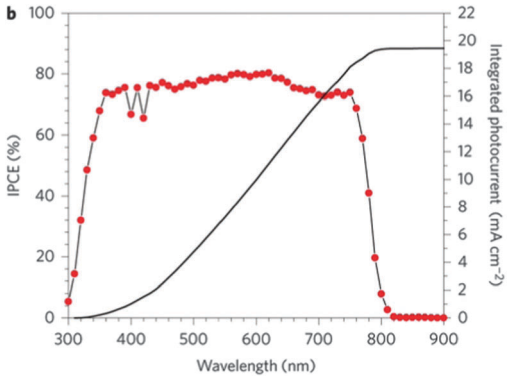

Fig. 16 IPCE spectrum of the MAPbI3 perovskite solar cell. The integrated product of the IPCE spectrum with the AM1.5G photon flux is also shown (black line). Reprinted by permission from Macmillan Publishers Ltd: [*Nature Photonics*] (ref. 137), copyright (2013).

with a heterojunction architecture. Optimal performances were observed for the PTAA devices, under a mp-TiO_2/$CH_3NH_3PbI_3$/PTAA configuration (V_{OC} of 0.997 V, J_{SC} of 16.5 mA cm^{-2} and PCE of 12%).[142] As well, very recently, efficiencies rose to 14.79% by the use of a novel carbazole-based HTM in conjuction with $CH_3NH_3PbI_3$.[143] This efficiency is the highest among devices with HTMs different than spiro-OMeTAD. On the other hand, three modified spiro-OMeTAD derivatives, bearing methoxy groups at different positions of the main structure, were prepared and evaluated as HTM in perovskite devices.[144] This adjustment of the HTM's electronic properties resulted in enhanced performances, with the *o*-substituted derivative giving the finest PCE of 16.7%.

Albeit the vibrant progress in the field there are still a number of scientific challenges involved in the further development of perovskite solar cells. Research is ongoing on (i) preparation of other TiO_2 structures (*e.g.*, nanorods) that facilitate pore filling of the HTM,[145] (ii) lowering the processing temperature to obtain cost-friendly techniques,[136,146,147] (iii) optimization of the efficiency in bulk heterojunction configurations.

5. Conclusions and perspectives

It is certain that new generation solar technologies will have a crucial role to play in attaining the ambitious goal of decoupling energy demand and carbon footprint from economic development. However, for enhancement of the relative competitiveness, further advances will be required. Questions such as cost, environmental impact, efficiency and scalability of the synthesis of active materials will play a key role in the industrial destiny of innovative photovoltaics.

In terms of all-organic photovoltaics, important developments in the last decade have led to very efficient devices reaching 12% overall conversion efficiencies (Table 1). Factors limiting device optimization involve primarily morphology, and significant efforts are being dedicated to improve current processing methods. As well, vivid interest is dedicated to the control of charge recombination by engineering the distance between donor and acceptor. On the other hand, device performance also highly depends on the optoelectronic properties of the active layer materials. Molecular design is primarily concerned with the rational chemical tuning of the sensitizer's molecular properties in order to achieve appropriate bandgaps to maximize the J_{SC} and V_{OC}, promote efficient charge carrier mobilities, optimal stacking characteristics, stability and solution processability.

As regards DSSCs, tremendous progress has resulted in 13% efficient devices today, attributed to critical selection and design of sensitizers and electrolytes (Table 1). Key points for further enhancement involve limit losses in potential and absorption/photocurrent. In this context, current research focuses on organic

Table 1 Photovoltaic parameters of the best performing solar cells based on the most efficient dyes

All-organic photovoltaics

Dye	Active layer	V_{OC} [V]	J_{SC} [mA cm^{-2}]	FF [%]	PCE [%]	Ref.
PTB7	PTB7:$PC_{70}BM$ (inverted cell – single junction)	0.75	17.46	69.99	9.2	31
PTB7-Th	PTB7-Th:$PC_{71}BM$ (inverted cell – single junction)	0.80	17.24	74.1	10.31	31*d*
PDTP-DFBT	P3HT:ICBA/PDTP-DFBT:$PC_{71}BM$ (tandem – double junction)	1.53	10.1	68.5	10.6	40
	P3HT:ICBA/PTB7:$PC_{71}BM$/PDTP-DFBT:$PC_{71}BM$ (tandem – triple junction)	2.28	7.63	66.39	11.5	42
SMPV1	SMPV1:$PC_{71}BM$ (tandem – double junction)	1.82	7.7	72.0	10.1	54

Dye-sensitized solar cells

Dye	Electrolyte	V_{OC} [V]	J_{SC} [mA cm^{-2}]	FF [%]	PCE [%]	Ref.
CYC-B11	I^-/I^{3-}	0.74	20.05	77.0	11.5	84
C219	I^-/I^{3-}	0.77	17.94	73.0	10.1	86
RK1	I^-/I^{3-}	0.76	18.26	74.0	10.2	87
SM315	$[Co(bpy)_3]^{2+/3+}$	0.91	18.1	78.0	13.0	75

Perovskite solar cells

Dye	HTM/cell structure	V_{OC} [V]	J_{SC} [mA cm^{-2}]	FF [%]	PCE [%]	Ref.
CH_3NH_3 $Pb(I_{1-x}Br_x)_3$	Poly(triarylamine)/bilayer architecture comprising mesoscopic and planar structures	1.11	19.64	74.2	16.2	141
$CH_3NH_3PbI_3$	spiro-OMeTAD derivative/mesoscopic TiO_2	1.02	21.2	77.6	16.7	144
$FAPbI_3$	spiro-OMeTAD/mesoscopic TiO_2	1.03	20.97	74.0	16.0	139
$CH_3NH_3PbI_{3-x}Cl_x$	spiro-OMeTAD/planar heterojunction	1.13	22.75	75.01	19.3	140

sensitizers with better light-harvesting capabilities and alignment of molecular orbitals, lower tendency to aggregate and photostability. Efforts in molecular design are concentrated in incorporating in common sensitizer units with light response in the NIR region, as well as long bulky chains. The latter can provide shielding of the TiO_2 surface from the redox mediator and avoid aggregate formation. As well, favorable interaction of the dye with the electrolyte is crucial, as it promotes rapid charge transfer of the hole to the redox couple. Introduction of suitable functional groups, in this respect, are investigated. Lastly, anchoring trends of the dyes towards enhanced electron injection are studied. Alternatively, intense efforts are dedicated in optimized liquid and solid electrolytes, improvement of the TiO_2 conductivity through morphological control, and counter electrodes of high corrosion resistance and reduction rate. The greatest challenge, however, other than the optimization of the individual materials of a device, is to reach a well-matched design, energetically and kinetically, able to optimize the overall device performance. It should be mentioned that tandem DSSC architectures are also envisaged as a powerful means towards panchromatic absorption.

Considering the pace of recent developments in both the OPV and DSSC fields, it is realistic to expect that the 15% threshold is not very far from becoming reality.

Lastly, the emerging perovskite-sensitized solar cells have been on a flourishing ride yielding prominent results, with the efficiencies blowing to 20.1% within 5 years (Table 1). The utilization of hybrid organic–inorganic perovskites offers both the advantages of organic compounds (solution processability and molecular engineering), and those of inorganic crystalline semiconductors (high charge mobilities and large absorption coefficients). One drawback of these materials is the use of lead, which is toxic and water sensitive, thus, an effort to replace it with less toxic elements is on-going. Alternatively, chemical modification of currently used perovskites, or even moving from single- to multijunction configurations are being considered, as a means to improve light harnessing and photocurrent. Morphology optimization (thickness and homogeneousity) is also an issue of concern, as is the search for alternative HTM with higher carrier mobilities. Finally, theoretical studies towards the elucidation of the operating principles of perovskite solar cells are of paramount importance and will certainly be highly beneficial to improve device performance. Considering the latest achievements and the room for optimization of current state-of-the art devices, an even more substantial increase in efficiencies seems like a realistic scenario.

In anticipation of continued improvements, envisioning an energy revolution that will be reflected in a high solar electricity future is no longer a longstanding goal. The scientific credibility of new generation photovoltaics is becoming stronger based on the impressive gains of current trends, however there remains plenty of scope for further improvement. After all, the race to harness sunlight still remains a formidable challenge.

Acknowledgements

Financial support is acknowledged from the European Union within the FP7-ENERGY-2012-1 framework, GLOBALSOL project, Proposal No 309194-2 and from the Spanish MEC and MICINN, Spain (CTQ2011-24187/BQU,PRI-PIBUS-2011-1128), and the Comunidad de Madrid (S2013/MIT-2841 FOTOCARBON).

Notes and references

1 IEA, *Energy Technology Perspectives (ETP)*, OECD/IEA, Paris, 2014.
2 N. S. Lewis and D. G. Nocera, *Proc. Natl. Acad. Sci. U. S. A.*, 2006, 15729–15735.
3 IEA, *Technology Roadmap. Solar photovoltaic energy*, OECD/IEA, Paris, 2010.
4 A. H. Tullo, *Chem. Eng. News*, 2010, **88**, 20–22.
5 S. A. Kalogirou, *Prog. Energy Combust. Sci.*, 2004, **30**, 231–295.
6 D. M. Chapin, C. S. Fuller and G. L. Pearson, *J. Appl. Phys.*, 1954, **25**, 676.
7 M. A. Green, *Philos. Trans. R. Soc., A*, 2013, 20110413.
8 M. A. Green, K. Emery, Y. Hishikawa, W. Warta and E. D. Dunlop, *Prog. Photovoltaics*, 2013, 827–837.
9 Goldman Sachs, *Goldman Sachs research report*, Goldman Sachs, New York, NY, 2011.
10 L. M. Peter, *Philos. Trans. R. Soc., A*, 2011, 1840–1856.
11 D. Kearns and M. J. Calvin, *Chem. Phys.*, 1958, **29**, 950.
12 (*a*) K. A. Mazzio and C. K. Luscombe, *Chem. Soc. Rev.*, 2015, **44**, 78–90; (*b*) C. J. Brabec, N. S. Sariciftci and J. C. Hummelen, *Adv. Funct. Mater.*, 2001, **11**, 15–26.
13 C. W. Tang, *Appl. Phys. Lett.*, 1986, **48**, 183.
14 T. Ameri, G. Dennler, C. Waldauf, H. Azimi, A. Seemann, K. Forberich, J. Hauch, M. Scharber, K. Hingerl and C. J. Brabec, *Adv. Funct. Mater.*, 2010, **20**, 1592–1598.
15 H. Spanggaard and F. C. Krebs, *Sol. Energy Mater. Sol. Cells*, 2004, **83**, 125–146.
16 (*a*) B. Qi and J. Wang, *J. Mater. Chem.*, 2012, **22**, 24315–24325; (*b*) M. S. Scharber, D. Mühlbacher, M. Koppe, P. Denk, C. Waldauf, A. J. Heeger and C. J. Brabec, *Adv. Mater.*, 2006, **18**, 789–794.
17 T. Umeyama and H. Imahori, *J. Mater. Chem. A*, 2014, **2**, 11545–11560.
18 Y. Huang, E. J. Kramer, A. J. Heeger and G. C. Bazan, *Chem. Rev.*, 2014, **114**, 7006–7043.
19 C. J. Brabec, S. Gowrisanker, J. J. M. Halls, D. Laird, S. Jia and S. P. Williams, *Adv. Mater.*, 2010, **22**, 3839–3856.
20 L. A. A. Petterson, L. S. Roman and O. Inganäs, *J. Appl. Phys.*, 1999, **86**, 487–496.
21 J. L. Delgado, P.-A. Bouit, S. Filippone, M. A. Herranz and N. Martín, *Chem. Commun.*, 2010, **46**, 4853–4865.
22 J. C. Hummelen, B. W. Knight, F. Lepec and F. Wudl, *J. Org. Chem.*, 1995, **60**, 532–538.
23 G. Yu, J. Gao, J. C. Hummelen, F. Wudl and A. J. Heeger, *Science*, 1995, **270**, 1789–1791.
24 (*a*) A. F. Eftaiha, J.-P. Sun, I. G. Hill and G. C. Welch, *J. Mater. Chem. A*, 2014, **2**, 1201–1213; (*b*) P. Sonar, J. P. F. Lim and K. L. Chan, *Energy Environ. Sci.*, 2011, **4**, 1558–1574; (*c*) C. L. Chochos, N. Tagmatarchis and V. G. Gregoriou, *RSC Adv.*, 2013, **3**, 7160–7181.
25 (*a*) X. Zhang, Z. Lu, L. Ye, C. Zhan, J. Hou, S. Zhang, B. Jiang, Y. Zhao, J. Huang, S. Zhang, Y. Liu, Q. Shi, Y. Liu and J. Yao, *Adv. Mater.*, 2013, **25**, 5791–5797; (*b*) E. Kozma and M. Catellani, *Dyes Pigm.*, 2013, **98**, 160–179; (*c*) X. Zhang, J. Yao and C. Zhan, *Chem. Commun.*, 2015, **51**, 1058–1061.
26 Y. Zang, C.-Z. Li, C.-C. Chueh, S. T. Williams, W. Jiang, Z.-H. Wang, J.-S. Yu and A. K.-Y. Jen, *Adv. Mater.*, 2014, **26**, 5708–5714.
27 Y. Zhong, M. T. Trinh, R. Chen, W. Wang, P. P. Khlyabich, B. Kumar, Q. Xu, C.-Y. Nam, M. Y. Sfeir, C. Black, M. L. Steigerwald, Y.-L. Loo, S. Xiao, F. Ng, X.-Y. Zhu and C. Nuckolls, *J. Am. Chem. Soc.*, 2014, **136**, 15215–15221.
28 M. M. Wienk, J. M. Kroon, W. J. H. Verhees, J. Knol, J. C. Hummelen, P. A. van Hal and R. A. J. Janssen, *Angew. Chem., Int. Ed.*, 2003, **42**, 3371–3375.

29 (*a*) W. Ma, C. Yang, X. Gong, K. Lee and A. J. Heeger, *Adv. Funct. Mater.*, 2005, **15**, 1617–1622; (*b*) J. Y. Kim, S. H. Kim, H.-H. Lee, K. Lee, W. Ma, X. Gong and A. J. Heeger, *Adv. Mater.*, 2006, **18**, 572–576.
30 G. Dennler, M. C. Scharber and C. J. Brabec, *Adv. Mater.*, 2009, **21**, 1323–1338.
31 (*a*) L. Lu and L. Yu, *Adv. Mater.*, 2014, **26**, 4413–4430; (*b*) Z. He, C. Zhong, X. Huang, W. Y. Wong, H. Wu, L. Chen, S. Su and Y. Cao, *Adv. Mater.*, 2011, **23**, 4636–4643; (*c*) J.-D. Chen, C. Cui, Y.-Q. Li, L. Zhou, Q.-D. Ou, C. Li, Y. Li and J.-X. Tang, *Adv. Mater.*, 2014, DOI: 10.1002/adma.201404535; (*d*) S.-H. Liao, H.-J. Jhuo, P.-N. Yeh, Y.-S. Cheng, Y.-L. Li, Y.-H. Lee, S. Sharma and S.-A. Chen, *Sci. Rep.*, 2014, **4**, 6813.
32 Z. He, C. Zhong, S. Su, M. Xu, H. Wu and Y. CaoSon, *Nat. Photonics*, 2012, **6**, 591–595.
33 S. Beaupré and M. Leclerc, *J. Mater. Chem. A*, 2013, **1**, 11097–11105.
34 S. H. Park, A. Roy, S. Beaupré, S. Cho, N. Coates, J. S. Moon, D. Moses, M. Leclerc, K. Lee and A. J. Heeger, *Nat. Photonics*, 2009, **3**, 297–303.
35 Y.-H. Chao, J.-F. Jheng, J.-S. Wu, K.-Y. Wu, H.-H. Peng, M.-C. Tsai, C.-L. Wang, Y.-N. Hsiao, C.-L. Wang, C.-Y. Lin and C.-S. Hsu, *Adv. Mater.*, 2014, **26**, 5205–5210.
36 (*a*) S. Sista, Z. R. Hong, L. M. Chen and Y. Yang, *Energy Environ. Sci.*, 2011, **4**, 1606–1620; (*b*) T. Ameri, G. Dennler, C. Lungenschmied and C. J. Brabec, *Energy Environ. Sci.*, 2009, **2**, 347–363; (*c*) A. Hadipour, B. de Boer and P. W. M. Blom, *Adv. Funct. Mater.*, 2008, **18**, 169–181; (*d*) J. You, L. Dou, Z. Hong, G. Li and Y. Yang, *Prog. Polym. Sci.*, 2013, **38**, 1909–1928; (*e*) O. Adebanjo, B. Vaagensmith and Q. Qiao, *J. Mater. Chem. A*, 2014, **2**, 10331–10349.
37 A. Yakimov and S. R. Forrest, *Appl. Phys. Lett.*, 2002, **80**, 1667.
38 A. De Vos, *J. Phys. D: Appl. Phys.*, 1980, **13**, 839.
39 J. Yang, R. Zhu, Z. Hong, Y. He, A. Kumar, Y. Li and Y. Yang, *Adv. Mater.*, 2011, **23**, 3465–3470.
40 J. You, L. Dou, K. Yoshimura, T. Kato, K. Ohya, T. Moriarty, K. Emery, C.-C. Chen, J. Gao, G. Li and Y. Yang, *Nat. Commun.*, 2013, **4**, 1446.
41 J. You, C.-C. Chen, Z. Hong, K. Yoshimura, K. Ohya, R. Xu, S. Ye, J. Gao, G. Li and Y. Yang, *Adv. Mater.*, 2013, **25**, 3973–3978.
42 C.-C. Chen, W.-H. Chang, K. Yoshimura, K. Ohya, J. You, J. Gao, Z. Hong and Y. Yang, *Adv. Mater.*, 2014, **26**, 5670–5677.
43 (*a*) O. Adebanjo, P. P. Maharjan, P. Adhikary, M. Wang, S. Yang and Q. Qiao, *Energy Environ. Sci.*, 2013, **6**, 3150–3170; (*b*) W. Li, A. Furlan, K. H. Hendriks, M. M. Wienk and R. A. Janssen, *J. Am. Chem. Soc.*, 2013, **135**, 5529–5532.
44 Newsletter Heliatek, January 16, 2013, http://www.heliatek.com/newscenter/latest_news/neuer-weltrekord-fur-organischesolarzellen-heliatek-behauptet-sich-mit-12-zelleffizienz-alstechnologiefuhrer/?lang=en.
45 J. Roncali, P. Frère, P. Blanchard, R. de Bettignies, M. Turbiez, S. Roquet, P. Leriche and Y. Nicolas, *Thin Solid Films*, 2006, **511**, 567–575.
46 J. Roncali, P. Leriche and P. Blanchard, *Adv. Mater.*, 2014, **26**, 3821–3838.
47 (*a*) J. Roncali, *Acc. Chem. Res.*, 2009, **42**, 1719–1730; (*b*) M. V. Martínez-Díaz, G. de la Torre and T. Torres, *Chem. Commun.*, 2010, **46**, 7090–7108.
48 A. Mishra and P. Bäuerle, *Angew. Chem., Int. Ed.*, 2012, **51**, 2020–2067.
49 B. Walker, C. Kim and T.-Q. Nguyen, *Chem. Mater.*, 2011, **23**, 470–482.
50 A. Mishra, C.-Q. Ma and P. Bäuerle, *Chem. Rev.*, 2009, **109**, 1141–1276.
51 R. Fitzner, E. Mena-Osteritz, A. Mishra, G. Schulz, E. Reinold, M. Weil, C. Körner, H. Ziehlke, C. Elschner, K. Leo, M. Riede, M. Pfeiffer, C. Uhrich and P. Bäuerle, *J. Am. Chem. Soc.*, 2012, **134**, 11064–11067.
52 J. E. Coughlin, J. B. Henson, G. C. Welch and G. C. Bazan, *Acc. Chem. Res.*, 2014, **47**, 257–270.
53 J. Zhou, Y. Zuo, X. Wan, G. Long, Q. Zhang, W. Ni, Y. Liu, Z. Li, G. He, C. Li, B. Kan, M. Li and Y. Chen, *J. Am. Chem. Soc.*, 2013, **135**, 8484–8487.
54 Y. Liu, C.-C. Chen, Z. Hong, J. Gao, Y. M. Yang, H. Zhou, L. Dou, G. Li and Y. Yang, *Sci. Rep.*, 2013, **3**, 3356.
55 S. Yoo, B. Domercq and B. Kippelen, *Appl. Phys. Lett.*, 2004, **85**, 5427–5429.
56 A. K. Pandey and J. M. Nunzi, *Adv. Mater.*, 2007, **19**, 3613–3617.
57 S. Wang, E. I. Mayo, M. D. Perez, L. Griffe, G. Wie, P. I. Djurovich, S. R. Forrest and M. E. Thompson, *Appl. Phys. Lett.*, 2009, **94**, 233304.
58 G. Wei, S. Wang, K. Sun, M. E. Thompson and S. R. Forrest, *Adv. Energy Mater.*, 2011, **1**, 184–187.
59 Y.-H. Chen, L.-Y. Lin, C.-W. Lu, F. Lin, Z.-Y. Huang, H.-W. Lin, P.-H. Wang, Y.-H. Liu, K.-T. Wong, J. Wen, D. J. Miller and S. B. Darling, *J. Am. Chem. Soc.*, 2012, **134**, 13616–13623.
60 V. Steinmann, N. M. Kronenberg, M. R. Lenze, S. M. Graf, D. Hertel, K. Meerholz, H. Bürckstümmer, E. V. Tulyakova and F. Würthner, *Adv. Energy Mater.*, 2011, **1**, 888–893.
61 V. Steinman, N. M. Kronenberg, M. R. Lenze, S. M. Graf, D. Hertel, H. Bürckstümmer, F. Würthner and K. Meerholz, *Appl. Phys. Lett.*, 2011, **99**, 193306.
62 S.-W. Chiu, L.-Y. Lin, H.-W. Lin, Y.-H. Chen, Z.-Y. Huang, Y.-T. Lin, F. Lin, Y.-H. Liu and K.-T. Wong, *Chem. Commun.*, 2012, **48**, 1857–1859.
63 B. Walker, A. B. Tamayo, X. D. Dang, P. Zalar, J. H. Seo, A. Garcia, M. Tantiwiwat and T.-Q. Nguyen, *Adv. Funct. Mater.*, 2009, **19**, 3063–3069.
64 J. Xue, S. Uchida, B. P. Rand and S. R. Forrest, *Appl. Phys. Lett.*, 2004, **84**, 3013–3015.
65 J. Xue, B. P. Rand, S. Uchida and S. R. Forrest, *Adv. Mater.*, 2005, **17**, 66–71.
66 J. Xue, S. Uchida, B. P. Rand and S. R. Forrest, *Appl. Phys. Lett.*, 2004, **85**, 5757–5759.
67 C. G. Claessens, D. González-Rodríguez, M. S. Rodríguez-Morgade, A. Medina and T. Torres, *Chem. Rev.*, 2014, **114**, 2192–2277.
68 R. Pandey, Y. Zou and R. J. Holmes, *Appl. Phys. Lett.*, 2012, **101**, 033308.
69 P. Sullivan, A. Duraud, I. Hancox, N. Beaumont, G. Mirri, J. H. R. Tucker, R. A. Hatton, M. Shipman and T. S. Jones, *Adv. Energy Mater.*, 2011, **1**, 352.
70 B. Verreet, K. Cnops, D. Cheyns, P. Heremans, A. Stesmans, G. Zango, C. G. Claessens, T. Torres and B. P. Rand, *Adv. Energy Mater.*, 2014, 1301413.
71 K. Cnops, B. P. Rand, D. Cheyns, B. Verreet, M. A. Empl and P. Heremans, *Nat. Commun.*, 2014, **5**, 3406.
72 (*a*) A. Hagfeldt, G. Boschloo, L. Sun, L. Kloo and H. Pettersson, *Chem. Rev.*, 2010, **110**, 6595–6663; (*b*) M. K. Nazeeruddin, E. Baranoff and M. Grätzel, *Sol. Energy*, 2011, **85**, 1172–1178.
73 B. O'Regan and M. Grätzel, *Nature*, 1991, **353**, 737–740.
74 H. S. Jung and J.-K. Lee, *J. Phys. Chem. Lett.*, 2013, **4**, 1682–1693.
75 S. Mathew, A. Yella, P. Gao, R. Humphry-Baker, B. F. E. Curchod, N. Ashari-Astani, I. Tavernelli, U. Rothlisberger, M. K. Nazeeruddin and M. Grätzel, *Nat. Chem.*, 2014, **6**, 242–247.
76 M. Grätzel, *Prog. Photovoltaics*, 2000, **8**, 171–185.
77 M. Grätzel, *Acc. Chem. Res.*, 2009, **42**, 1788–1798.
78 B. E. Hardin, H. J. Snaith and M. D. McGehee, *Nat. Photonics*, 2012, **6**, 162–169.
79 L. Giribabu, R. K. Kanaparthi and V. Velkannan, *Chem. Rec.*, 2012, **12**, 306–328.
80 M. Nazeeruddin, A. Kay, I. Rodicio, R. Humphry-Baker, E. Muller, P. Liska, N. Vlachopoulos and M. Grätzel, *J. Am. Chem. Soc.*, 1993, **115**, 6382–6390.
81 M. Nazeeruddin, S. Zakeeruddin, R. Humphry-Baker, M. Jirousek, P. Liska, N. Vlachopoulos, V. Shklover, C. Fischer and M. Grätzel, *Inorg. Chem.*, 1999, **38**, 6298–6305.
82 M. Nazeeruddin, P. Pechy, T. Renouard, S. Zakeeruddin, R. Humphry-Baker, P. Comte, P. Liska, L. Cevey, E. Costa, V. Shklover, L. Spiccia, G. Deacon, C. Bignozzi and M. Grätzel, *J. Am. Chem. Soc.*, 2001, **123**, 1613–1624.
83 J.-F. Yin, M. Velayudham, D. Bhattacharya, H.-C. Lin and K.-L. Lu, *Coord. Chem. Rev.*, 2012, **256**, 3008–3035.
84 C.-Y. Chen, M. Wang, J.-Y. Li, N. Pootrakulchote, L. Alibabaei, C.-H. Ngoc-le, J. D. Decoppet, J.-H. Tsai, C. Grätzel, C.-G. Wu, S. M. Zakeeruddin and M. Grätzel, *ACS Nano*, 2009, **3**, 3103–3109.
85 (*a*) J. N. Clifford, M. Planells and E. Palomares, *J. Mater. Chem.*, 2012, **22**, 24195–24201; (*b*) A. Mishra, M. K. R. Fischer and P. Bäuerle, *Angew. Chem., Int. Ed.*, 2009, **48**, 2474–2499.

86 W. Zeng, Y. Cao, Y. Bai, Y. Wang, Y. Shi, M. Zhang, F. Wang, C. Pan and P. Wang, *Chem. Mater.*, 2010, **22**, 1915–1925.
87 D. Joly, L. Pellejà, S. Narbey, F. Oswald, J. Chiron, J. N. Clifford, E. Palomares and R. Demadrille, *Sci. Rep.*, 2014, **4**, 4033.
88 (*a*) M. Urbani, M. Grätzel, M. K. Nazeeruddin and T. Torres, *Chem. Rev.*, 2014, **114**, 12330–12396; (*b*) L.-L. Li and E. W.-G. Diau, *Chem. Soc. Rev.*, 2013, **42**, 291–304.
89 A. Yella, H. W. Lee, H. N. Tsao, C. Yi, A. K. Chandiran, M. K. Nazeeruddin, E. W.-G. Diau, C. Y. Yeh, S. M. Zakeeruddin and M. Grätzel, *Science*, 2011, **334**, 629–634.
90 A. Yella, C.-L. Mai, S. M. Zakeeruddin, S.-N. Chang, C.-H. Hsieh, C.-Y. Yeh and M. Grätzel, *Angew. Chem., Int. Ed.*, 2014, **53**, 2973–2977.
91 (*a*) V. K. Singh, R. K. Kanaparthi and L. Giribabu, *RSC Adv.*, 2014, **4**, 6970–6984; (*b*) L. Martín-Gomis, F. Fernández-Lázaro and A. Sastre-Santos, *J. Mater. Chem. A*, 2014, **2**, 15672–15682; (*c*) M. E. Ragoussi, M. Ince and T. Torres, *Eur. J. Org. Chem.*, 2013, 6475–6489.
92 J.-J. Cid, J.-H. Yum, S.-R. Jang, M. K. Nazeeruddin, E. Martínez-Ferrero, E. Palomares, J. Ko, M. Grätzel and T. Torres, *Angew. Chem., Int. Ed.*, 2007, **46**, 8358–8362.
93 S. Mori, M. Nagata, Y. Nakahata, K. Yasuta, R. Goto, M. Kimura and M. Taya, *J. Am. Chem. Soc.*, 2010, **132**, 4054–4055.
94 (*a*) M. E. Ragoussi, J. J. Cid, J. H. Yum, G. de la Torre, D. Di Censo, M. Grätzel, M. K. Nazeeruddin and T. Torres, *Angew. Chem., Int. Ed.*, 2012, **51**, 4375–4378 (*Angew. Chem.*, 2012, **124**, 4451–4454); (*b*) M. E. Ragoussi, J. H. Yum, A. K. Chandiran, M. Ince, G. de La Torre, M. Grätzel, M. K. Nazeeruddin and T. Torres, *ChemPhysChem*, 2014, **15**, 1033–1036.
95 B. C. O'Regan, I. López-Duarte, M. V. Martínez-Díaz, A. Forneli, J. Albero, A. Morandeira, E. Palomares, T. Torres and J. R. Durrant, *J. Am. Chem. Soc.*, 2008, **130**, 2906–2907.
96 T. Ikeuchi, H. Nomoto, N. Masaki, M. J. Griffith, S. Mori and M. Kimura, *Chem. Commun.*, 2014, **50**, 1941–1943.
97 A. Hagfeldt and M. Grätzel, *Chem. Rev.*, 1995, **95**, 49–68.
98 Z. S. Wang, K. Sayama and H. Sugihara, *J. Phys. Chem. B*, 2005, **109**, 22449–22455.
99 K. Hara, T. Horiguchi, T. Kinoshita, K. Sayama and H. Arakawa, *Sol. Energy Mater. Sol. Cells*, 2001, **70**, 151–161.
100 F. Pichot and B. A. Gregg, *J. Phys. Chem. B*, 2000, **104**, 6–10.
101 T. Daeneke, T. H. Kwon, A. B. Holmes, N. W. Duffy, U. Bach and L. Spiccia, *Nat. Chem.*, 2011, **3**, 211–215.
102 (*a*) M. Wang, N. Chamberland, L. Breau, J.-E. Moser, R. Humphry-Baker, B. Marsan, S. M. Zakeeruddin and M. Grätzel, *Nat. Chem.*, 2010, **2**, 385–389; (*b*) H. Tian, Z. Yu, A. Hagfeldt, L. Kloo and L. Sun, *J. Am. Chem. Soc.*, 2011, **133**, 9413–9422.
103 S. M. Feldt, E. A. Gibson, E. Gabrielsson, L. Sun, G. Boschloo and A. Hagfeldt, *J. Am. Chem. Soc.*, 2010, **132**, 16714–16724.
104 J. H. Yum, E. Baranoff, F. Kessler, T. Moehl, S. Ahmad, T. Bessho, A. Marchioro, E. Ghadiri, J. E. Moser, C. Yi, M. K. Nazeeruddin and M. Grätzel, *Nat. Commun.*, 2012, **3**, 631.
105 D. Zhou, Q. Yu, N. Cai, Y. Bai, Y. Wanga and P. Wang, *Energy Environ. Sci.*, 2011, **4**, 2030–2034.
106 M. K. Kashif, M. Nippe, N. W. Duffy, C. M. Forsyth, C. J. Chang, J. R. Long, L. Spiccia and U. Bach, *Angew. Chem., Int. Ed.*, 2013, **52**, 5527–5531.
107 P. Docampo, S. Guldin, T. Leijtens, N. K. Noel, U. Steiner and H. J. Snaith, *Adv. Mater.*, 2014, **26**, 4013–4030.
108 U. Bach, Y. Tachibana, J.-E. Moser, S. A. Haque, J. R. Durrant, M. Grätzel and D. R. Klug, *J. Am. Chem. Soc.*, 1999, **121**, 7445–7446.
109 I. Chung, B. Lee, J. He, R. P. H. Chang and M. G. Kanatzidis, *Nature*, 2012, **485**, 486–489.
110 P. Chen, J.-H. Yum, F. De Angelis, E. Mosconi, S. Fantacci, S.-J. Moon, R. Humphry-Baker, J. Ko, M. K. Nazeeruddin and M. Grätzel, *Nano Lett.*, 2009, **9**, 2487–2492.
111 U. Bach, D. Lupo, P. Comte, J. E. Moser, F. Weissörtel, J. Salbeck, H. Spreitzer and M. Grätzel, *Nature*, 1998, **395**, 583–585.
112 J. Burschka, A. Dualeh, F. Kessler, E. Baranoff, N.-L. Cevey-Ha, C. Yi, M. K. Nazeeruddin and M. Grätzel, *J. Am. Chem. Soc.*, 2011, **133**, 18042–18045.
113 M. Pagliaro, G. Palmisano, R. Ciriminna and V. Loddo, *Energy Environ. Sci.*, 2009, **2**, 838–844.
114 Q. Zhang, C. S. Dandeneau, X. Zhou and G. Cao, *Adv. Mater.*, 2009, **21**, 4087–4108.
115 S. Ferrere, A. Zaban and B. A. Gregg, *J. Phys. Chem. B*, 1997, **101**, 4490–4493.
116 P. Guo and M. A. Aegerter, *Thin Solid Films*, 1999, 290–294.
117 (*a*) K. Sayama, S. Tsukagoshi, T. Mori, K. Hara, Y. Ohga, A. Shinpou, Y. Abe, S. Suga and H. Arakawa, *Sol. Energy Mater. Sol. Cells*, 2003, **80**, 47–71; (*b*) T. Chen, Z. Zeng, C. Li, W. Wang, X. Wang and B. Zhang, *New J. Chem.*, 2005, **29**, 773–776; (*c*) J.-H. Yum, S.-R. Jang, P. Walter, T. Geiger, F. Nüesch, S. Kim, J. Ko, M. Grätzel and M. K. Nazeeruddin, *Chem. Commun.*, 2007, 4680–4682.
118 (*a*) A. Ehret, L. Stuhi and M. T. Spitler, *J. Phys. Chem. B*, 2001, **105**, 9960–9965; (*b*) H. Otaka, M. Kira, K. Yano, S. Ito, H. Mitekura, T. Kawata and F. Matsui, *J. Photochem. Photobiol., A*, 2004, **164**, 67–73; (*c*) V. P. S. Perera, P. K. D. D. P. Pitigala, M. K. I. Senevirathne and K. Tennakone, *Sol. Energy Mater. Sol. Cells*, 2005, **85**, 91–98; (*d*) C. Siegers, U. Würfel, M. Zistler, H. Gores, J. Hohl-Ebinger, A. Hinsch and R. Haag, *ChemPhysChem*, 2008, **9**, 793–798.
119 J. Lakowicz, *Principles of Fluorescence Spectroscopy*, Springer, New York, 2010, pp. 1–33.
120 B. W. Hardin, E. T. Hoke, P. B. Armstrong, J.-H. Yum, P. Comte, T. Torres, J. M. Frechet, M. K. Nazeeruddin, M. Grätzel and M. D. McGehee, *Nat. Photonics*, 2009, **3**, 406–411.
121 J.-H. Yum, B. E. Hardin, E. T. Hoke, E. Baranoff, S. M. Zakeeruddin, M. K. Nazeeruddin, T. Torres, M. D. McGehee and M. Grätzel, *ChemPhysChem*, 2011, **12**, 657–661.
122 B. E. Hardin, J.-H. Yum, E. T. Hoke, Y. C. Jun, P. Pechy, T. Torres, M. L. Brongersma, Md. K. Nazeeruddin, M. Grätzel and D. McGehee, *Nano Lett.*, 2010, **10**, 3077–3083.
123 G. Y. Margulis, B. Lim, B. E. Hardin, E. L. Unger, J. H. Yum, J. M. Feckl, D. Fattakhova-Rohlfing, T. Bein, M. Grätzel, A. Sellinger and M. D. McGehee, *Phys. Chem. Chem. Phys.*, 2013, **15**, 11306–11312.
124 (*a*) S. Kazim, M. K. Nazeeruddin, M. Grätzel and S. Ahmad, *Angew. Chem., Int. Ed.*, 2014, **53**, 2812–2824; (*b*) M. He, D. Zheng, M. Wang, C. Linb and Z. Lin, *J. Mater. Chem. A*, 2014, **2**, 5994–6003; (*c*) P. Gao, M. Grätzel and M. K. Nazeeruddin, *Energy Environ. Sci.*, 2014, **7**, 2448–2463; (*d*) G. Giorgi and K. Yamashita, *J. Mater. Chem. A*, 2015, DOI: 10.1039/C4TA05046K; (*e*) M. A. Green, A. Ho-Baillie and H. J. Snaith, *Nat. Photonics*, 2014, **8**, 506–514; (*f*) T. Salim, S. Sun, Y. Abe, A. Krishna, A. C. Grimsdale and Y.-M. Lam, *J. Mater. Chem. A*, 2014, DOI: 10.1039/C4TA05226A; (*g*) G. Niu, X. Guo and L. Wan, *J. Mater. Chem. A*, 2015, DOI: 10.1039/C4TA04994B.
125 Science News, *Science*, 2013, **342**, 1438.
126 D. B. Mitzi, *J. Chem. Soc., Dalton Trans.*, 2001, 1–12.
127 A. Kojima, K. Teshima, Y. Shirai and T. Miyasaka, *J. Am. Chem. Soc.*, 2009, **131**, 6050–6051.
128 J. H. Im, C. R. Lee, J. W. Lee, S. W. Park and N. G. Park, *Nanoscale*, 2011, **3**, 4088–4093.
129 W. Li, J. Li, L. Wang, G. Niu, R. Gao and Y. Qiu, *J. Mater. Chem. A*, 2013, **1**, 11735–11740.
130 http://www.nrel.gov/ncpv/images/efficiency_chart.jpg.
131 J. H. Noh, N. J. Jeon, Y. C. Choi, M. K. Nazeeruddin, M. Grätzel and S. I. Seok, *J. Mater. Chem. A*, 2013, **1**, 11842–11847.
132 L. Etgar, P. Gao, Z. Xue, Q. Peng, A. K. Chandiran, B. Liu, M. K. Nazeeruddin and M. Grätzel, *J. Am. Chem. Soc.*, 2012, **134**, 17396–17399.
133 M. M. Lee, J. Teuscher, T. Miyasaka, T. N. Murakami and H. J. Snaith, *Science*, 2012, **338**, 643–647.
134 J. Burschka, N. Pellet, S. J. Moon, H. R. Baker, P. Gao, M. K. Nazeeruddin and M. Grätzel, *Nature*, 2013, **499**, 316–319.
135 M. Liu, M. B. Johnston and H. J. Snaith, *Nature*, 2013, **501**, 395–398.
136 J. M. Ball, M. M. Lee, A. Hey and H. J. Snaith, *Energy Environ. Sci.*, 2013, **6**, 1739–1743.
137 D. Liu and T. L. Kelly, *Nat. Photonics*, 2013, **8**, 133–138.
138 G. E. Eperon, S. D. Stranks, C. Menelaou, M. B. Johnston, L. M. Herz and H. J. Snaith, *Energy Environ. Sci.*, 2014, **7**, 982–988.
139 J.-W. Lee, D.-J. Seol, A.-N. Cho and N.-G. Park, *Adv. Mater.*, 2014, **26**, 4991–4998.
140 H. Zhou, Q. Chen, G. Li, S. Luo, T.-B. Song, H.-S. Duan, Z. Hong, J. You, Y. Liu and Y. Yang, *Science*, 2014, **345**, 542–546.
141 N. J. Jeon, J. H. Noh, Y. C. Kim, W. S. Yang, S. Ryu and S. I. Seok, *Nat. Mater.*, 2014, **13**, 897–903.

142 J. H. Heo, S. H. Im, J. H. Noh, T. N. Mandal, C. S. Lim, J. A. Chang, Y. H. Lee, H. J. Kim, A. Sarkar, M. K. Nazeeruddin, M. Grätzel and S. I. Seok, *Nat. Photonics*, 2013, **7**, 486–491.
143 S. D. Sung, M. S. Kang, I. T. Choi, H. M. Kim, H. Kim, M. Hong, H. K. Kim and W. I. Lee, *Chem. Commun.*, 2014, **50**, 14161–14163.
144 N. J. Jeon, H. G. Lee, Y. C. Kim, J. Seo, J. H. Noh, J. Lee and S. I. Seok, *J. Am. Chem. Soc.*, 2014, **136**, 7837–7840.
145 H. S. Kim, J. W. Lee, N. Yantara, P. P. Boix, S. A. Kulkarni, S. Mhaisalkar, M. Grätzel and N. G. Park, *Nano Lett.*, 2013, **13**, 2412–2417.
146 C. Y. Jiang, W. L. Koh, M. Y. Leung, S. Y. Chiam, J. S. Wu and J. Zhang, *Appl. Phys. Lett.*, 2012, **100**, 113901.
147 K. Wojciechowski, M. Saliba, T. Leijtens, A. Abatea and H. J. Snaith, *Energy Environ. Sci.*, 2014, **7**, 1142–1147.